

---

Masters Theses

Student Theses and Dissertations

---

1972

## Transient cooling of a sphere due to boiling

Salil K. Banerjee

Follow this and additional works at: [https://scholarsmine.mst.edu/masters\\_theses](https://scholarsmine.mst.edu/masters_theses)



Part of the [Mechanical Engineering Commons](#)

Department:

---

### Recommended Citation

Banerjee, Salil K., "Transient cooling of a sphere due to boiling" (1972). *Masters Theses*. 5051.  
[https://scholarsmine.mst.edu/masters\\_theses/5051](https://scholarsmine.mst.edu/masters_theses/5051)

This thesis is brought to you by Scholars' Mine, a service of the Missouri S&T Library and Learning Resources. This work is protected by U. S. Copyright Law. Unauthorized use including reproduction for redistribution requires the permission of the copyright holder. For more information, please contact [scholarsmine@mst.edu](mailto:scholarsmine@mst.edu).

TRANSIENT COOLING OF A SPHERE  
DUE TO BOILING

BY

SALIL KUMAR BANDYOPADHYAY, 1943-  
(BANERJEE)

A THESIS

Presented to the Faculty of the Graduate School of the

UNIVERSITY OF MISSOURI - ROLLA

In Partial Fulfillment of the Requirements for the Degree

MASTER OF SCIENCE IN MECHANICAL ENGINEERING

1972

T2707  
86 pages  
c. I

Approved by

A. L. Cosbri (Advisor)      L. J. Grimm  
Lyle G. Phee

ACKNOWLEDGEMENTS

The author wishes to express his sincere thanks and appreciation to his major professor Dr. A. L. Crosbie for his skilful guidance throughout this study. Dr. Crosbie unsparingly devoted much of his time from a busy schedule at every stage of this work. The author also gratefully acknowledges the encouragement received from Dr. L. G. Rhea and Dr. L. J. Grimm during this study who also acted as the second and third reader respectively. Gratitude is expressed to the faculty of the Mechanical Engineering Department of the University of Missouri-Rolla who made the computer facilities available for this analysis. The author wants to thank Mrs. Yvonne Hays who is responsible for the typing of this manuscript.

Finally a special appreciation is conveyed to Professor Ralph E. Schowalter of the mechanical engineering department and Mr. Louis Moss of the student personnel department who have been helpful to this author in many ways during his graduate work.

TABLE OF CONTENTS

	Page
ACKNOWLEDGEMENTS.....	ii
LIST OF FIGURES.....	iv
NOMENCLATURE.....	vi
ABSTRACT.....	viii
I. INTRODUCTION.....	1
II. REVIEW OF LITERATURE.....	8
A. Discussion.....	8
B. Tabular Form.....	13
III. MATHEMATICAL FORMULATION OF THE PROBLEM.....	16
IV. SOLUTIONS OF THE INTEGRAL EQUATION.....	24
A. Modified Successive Approximation Method.....	24
B. Separable Kernel Method.....	31
C. Modified Separable Kernel Method.....	36
V. RESULTS.....	39
VI. CONCLUSIONS.....	68
VII. BIBLIOGRAPHY.....	72
VIII. VITA.....	77

LIST OF FIGURES

Figures	Page
1. (a) Typical Heat Transfer Coefficient versus Surface Temperature Curve.....	4
(b) Typical Cooling Curve.....	4
2. Typical Variation of Surface Heat Flux with the Temperature Difference between the surface of the Solid and the Fluid in Transient Pool Boiling.....	5
3. Variation of Heat Transfer Coefficient with Surface Temperature as used in this analysis.....	19
4. Surface Temperature Distribution during the Cooling of a Sphere for both Infinite Thermal Conductivity and Exact Solutions for Different Biot Numbers ( $Bi = .5, 1, 5$ and $10$ ).....	41
5. Variation of Surface Temperature with the product of Biot Number and Time ( $Bi = 5$ and $10, k = \infty$ case).....	43
6. Comparison between the Exact Solution and Separable Kernel Approximations ( $Bi = .1$ ).....	44
7. Comparison between the Exact Solution and Separable Kernel Approximations ( $Bi = .5$ ).....	45
8. Comparison between the Exact Solution and Separable Kernel Approximations ( $Bi = .5, \text{large scale}$ ).....	46
9. Comparison between the Exact Solution and Separable Kernel Approximations ( $Bi = 1$ ).....	47
10. Comparison between the Exact Solution and Separable Kernel Approximations ( $Bi = 1, \text{large scale}$ ).....	48
11. Comparison between the Exact Solution and Separable Kernel Approximations ( $Bi = 1, \text{large scale with some Modified Separable Kernel Method Solutions}$ ).....	49
12. Comparison between the Exact Solution and Separable Kernel Approximations ( $Bi = 5$ ).....	50
13. Comparison between the Exact Solution and Separable Kernel Approximations ( $Bi = 10$ ).....	51

Figure	Page
14. Variation of Heat Flux with Surface Temperature ( $Bi = .5$ and $5$ ).....	56
15. Variation of Heat Flux with Surface Temperature ( $Bi = 1$ and $10$ ).....	57
16. Time Rate of Change of the Surface Temperature with Time for both the Exact and Infinite Thermal Conductivity Case ( $Bi = .1$ ).....	60
17. Variation of the Time Rate of Change of the Surface Temperature with Time for both the Exact and Infinite Thermal Conductivity Case ( $Bi = .5$ ).....	61
18. Variation of the Time Rate of Change of the Surface Temperature with Time for both the Exact and Infinite Thermal Conductivity Case ( $Bi = 1$ ).....	62
19. Variation of the Time Rate of Change of the Surface Temperature with Time for both the Exact and Infinite Thermal Conductivity Case ( $Bi = 5$ ).....	63
20. Variation of the Time Rate of Change of the Surface Temperature with Time for both the Exact and Infinite Thermal Conductivity Case ( $Bi = 10$ ).....	64

NOMENCLATURE

$c_p$	specific heat at constant pressure, Btu/lbm $^{\circ}\text{F}$
$g$	dimensionless surface heat flux
$h$	heat transfer coefficient, Btu/hr ft <sup>2</sup> $^{\circ}\text{F}$
$h_{\text{max}}$	maximum heat transfer coefficient, Btu/hr ft <sup>2</sup> $^{\circ}\text{F}$
$k$	thermal conductivity, Btu/hr ft $^{\circ}\text{F}$
$Bi$	Biot number $h_{\text{max}} R/k$ in case of variable $h$ and $h R/k$ in case of constant $h$
$r$	one dimensional spherical coordinate
$R$	radius of the sphere
$s$	variable used for Laplace transformation
$T$	absolute temperature
$T_f$	fluid temperature
$T_i$	initial temperature of the solid
$T_s$	surface temperature of the solid
$t$	dimensionless time $\alpha t_1/R^2$ or Fourier number
$t_1$	time
$u$	dimensionless temperature, $T/T_1$
$u_s$	dimensionless surface temperature, $T_s/T_1$
$w_1$	Gaussian weights
$w_1^{(2n)}$	Gaussian weights of order $2n$
$x_i$	Gaussian abscissa
$Y$	dimensionless surface temperature = $u_s$
$\alpha$	thermal diffusivity, ft <sup>2</sup> /hr
$\epsilon$	weighted coefficient for the temperature term in the modified separable kernel method
$\rho$	mass density, lbm/ft <sup>3</sup>

## Nomenclature (con't)

$\theta_c$	$T_f/T_i$
$\lambda$	eigenvalue



ABSTRACT

Bandyopadhyay, Salil K., University of Missouri at Rolla, Rolla, January, 1972. Transient Cooling of a Sphere due to Boiling.

Major Professor: Alfred L. Crosbie

The time - dependent surface temperature is determined for a sphere subjected to cooling by boiling. One dimensional heat transfer is considered and the solid is assumed to be homogeneous, isotropic and opaque to thermal radiation and to have temperature - independent physical properties. The initial temperature of the sphere and the coolant are assumed to be uniform and arbitrary. The boiling heat transfer coefficient at the surface of a sphere is a strong function of the surface temperature thus resulting in an extremely nonlinear transient heat conduction problem. As a practical application of the problem, the process of quenching has been cited.

In the analysis, the transient heat conduction equation with its initial and boundary conditions is transformed to a singular nonlinear Volterra integral equation of the second kind by use of the Laplace transformations. The equation is solved numerically on a digital computer by the method of modified successive approximations for the sphere. The time scale is broken into a desired number of intervals. The solution for the first time interval is obtained by successive approximations and then used in finding the solution for the next time interval. Initial guesses are obtained by the use of the ideal case of infinite thermal conductivity. The process of successive approximation is continued along the time scale till the solution

for all desired time is obtained. Within the limitations of the basic assumptions, the method can be termed as exact, since any degree of accuracy can be obtained. The results are presented in graphical and tabular forms and compared with analytical and experimental results where available.

A separable kernel method is also applied for the solution of the Volterra integral equation describing the surface temperature. The kernel of the integral equation is approximated by a simple expression and substituted in the original integral equation. By suitable mathematical techniques, the integral equation is then transformed to a differential equation which is much simpler to solve than the integral equation. The better the kernel is approximated, the more the separable kernel solution tends towards the solution obtained by the successive approximation method. This method of solution is more convenient to apply than the successive approximation method, but is not very accurate for Biot numbers greater than ten. Another approximate method, termed as the modified separable kernel method, is also presented for the solution of the integral equation. The accuracy of the modified method seems to be much better than the ordinary one and is found to give results within five percent of the exact solution when the kernel is represented by a suitable number of equations.

Limiting cases of large and small Biot numbers ( 0.1 to 10.0 ) are calculated and analysed in terms of the present solutions. It is concluded that the infinite thermal conductivity approach can approximate the exact solution to within ten percent for Biot numbers less than one.

## I INTRODUCTION

When a hot solid is suddenly immersed in a pool of cool liquid, transient pool boiling takes place. During the cooling process, three distinct stages of boiling heat transfer occur, namely film, transition and nucleate boiling. When the solid cools down to a temperature close to the saturation temperature of the liquid, heat is transferred by free convection until the system attains an equilibrium temperature. The heat transfer coefficient for all the regimes of boiling is a strong function of surface temperature which makes the governing boundary condition extremely nonlinear. Hence a general solution for the surface temperature of the sphere, valid for the entire cooling range seems difficult to obtain. Although transient pool boiling has been studied extensively, no exact solution for the surface temperature of a sphere has been presented so far.

Quenching is an excellent example of transient pool boiling and is widely used in different industries. In the fields of metallurgy and manufacturing, quenching is a hardening process. Initially, the metallurgists were primarily interested in obtaining a desirable hardness of the solid and little attention was given to the heat transfer problem associated with it. But due to the excellent work of Stolz, Paschkis et. al., [1], it has been conclusively proved that the investigation of heat transfer is necessary to achieve a desired hardness by quenching. In other words, a knowledge of the temperature history is useful in regulating the hardness.

For a better understanding of the relationship between the hardness and the heat transfer rate, a brief description of how quenching imparts hardness seems appropriate. When a solid is gradually heated in a furnace, beyond a certain temperature, structural changes take place in the solid. The range of temperature during which this transformation takes place is known as the critical range [2]. If the solid is then cooled down slowly, a reversible metallurgical transformation takes place as the body passes through the critical region and is transformed back to the original structure below this region. No noticeable change in the physical properties of the solid is observed after this process.

But if the hot solid is quenched, rapid cooling makes the process metallurgically irreversible. The solid does not have enough time to transform back to the original preheated structure. Instead, there is a distortion of the crystal lattice and a new structure (Martensite, in case of carbon steel) is formed. This new structure is responsible for the increased hardness of the solid. However, the structure is brittle and, therefore, vulnerable to shocks and breakage. An extremely rapid cooling rate will produce a high degree of hardness and at the same time will make the material extremely brittle, sometimes causing cracks to appear in the surface. Hence, the rate of cooling must be properly controlled to get the desirable compromise between hardness and brittleness.

The rate at which the solid cools is a strong function of the heat transfer coefficient which again is strongly related to the surface temperature. Thus, for control of the hardness, a knowledge

of the entire temperature history of the quenched solid is essential. Typical cooling rates (temperature - time) and heat transfer coefficient - temperature curves are shown in Figures (1a) and (1b), Reference [3].

It has been stated in the introductory paragraph that transient pool boiling encompasses three distinct regimes of boiling. A brief description of each of these regimes is now given. In film boiling, the temperature difference between the solid and the liquid is large and a vapor film completely surrounds the solid. In this stage, the vapor film acts as the medium of heat transfer between the solid and the liquid. This regime of boiling is shown by the portion ab in the curve in Figure (2). As the cooling continues, transition boiling occurs. This state of boiling is unstable and characterized by the alternate formation of vapor films and agitated vapor bubbles at different locations of the heating surface. Within this region, the amount of vapor generated is not enough to support a stable vapor film over the entire surface but is again too large to allow a sufficient amount of liquid to reach the surface for creating enough bubbles for nucleate boiling (discussed later). This phase of boiling is marked by the dashed portion bc of the curve in Figure (2).

With a further drop in temperature difference, the formation of a continuous stream of bubbles is observed on the heat transfer surface. The above phenomenon occurs in the nucleate boiling regime. This regime of boiling is shown by cd on the curve in Figure (2). In the first part of this regime the vapor bubbles are large whereas in the later part, with a further reduction in the temperature of the solid, the bubbles become smaller and less numerous than those in

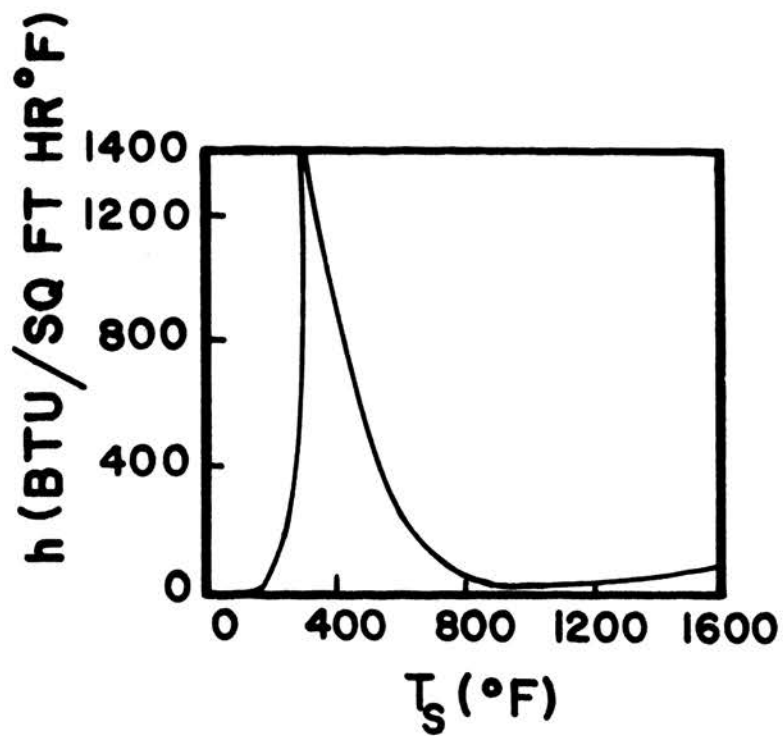


Fig. 1(a) Typical Heat Transfer Coefficient versus Surface Temperature Curve.

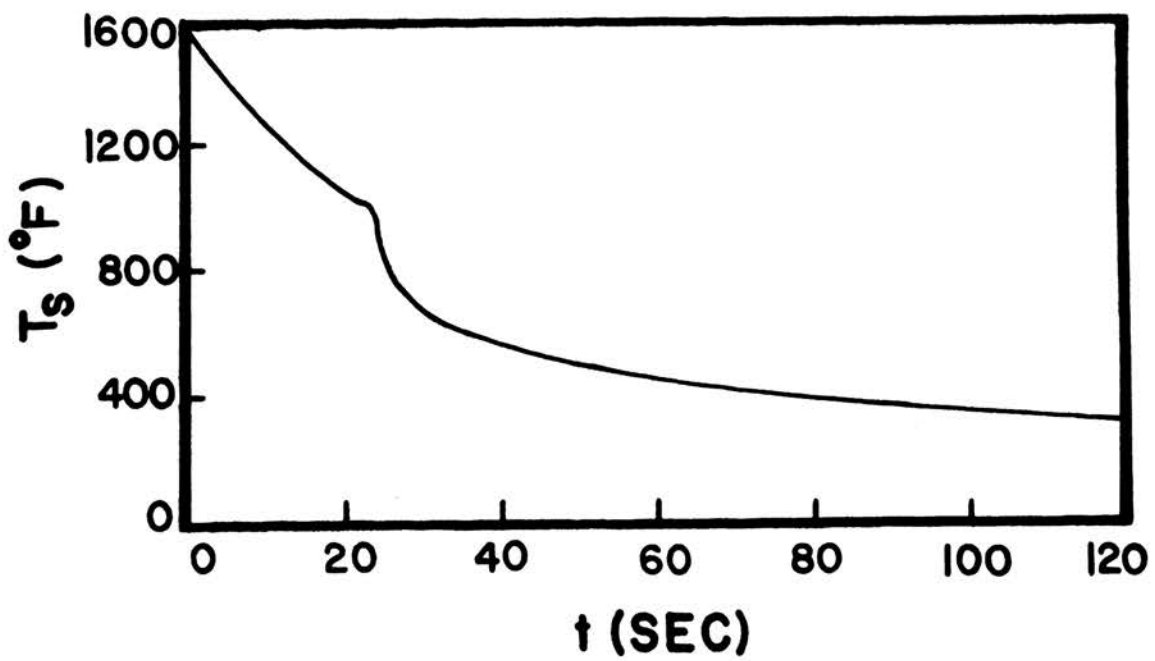


Fig. 1(b) Typical Cooling Curve.

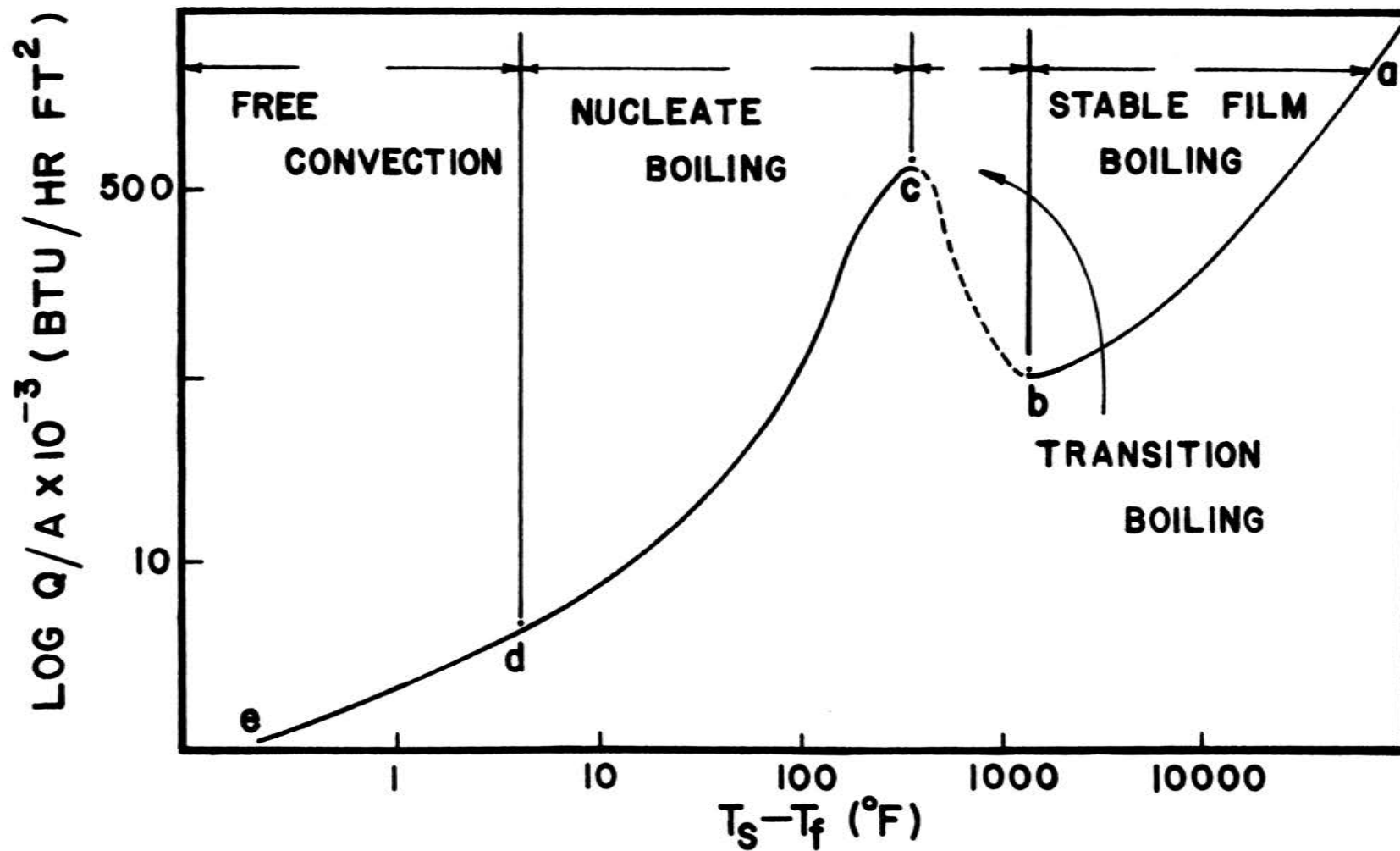


Fig. 2 Typical Variation of Surface Heat Flux with the Temperature Difference between the surface of the Solid and the Fluid in Transient Pool Boiling.

the earlier part and condense before reaching the surface of the subcooled liquid. There are many theories about the formation of bubbles (nucleation). However, most of the theories suggest the existence of the "nucleation sites" on the heating surface from which the bubbles originate. It is to be observed that although the temperature difference between the solid and the liquid in the nucleate boiling regime is less than that in the film boiling regime, the heat flux in some portion of the nucleate boiling regime is higher than that in the film boiling regime.

Finally when the surface temperature is close to the saturation temperature of the liquid (considering subcooled liquid), transfer of heat takes place by free convection. In this regime the heat transfer coefficient is proportional to the temperature difference between the solid and the liquid to the one fourth power. This region is shown by de on the curve in Figure (2).

Unfortunately, a simple relation between the heat transfer coefficient and the temperature difference between the solid and the liquid, as exists in the case of laminar free convection, does not seem to exist for boiling heat transfer, connecting all the regimes of boiling. Some correlations between the heat transfer coefficient and the temperature difference do exist for film and nucleate boiling. But these correlations are valid strictly for the particular regime and the conditions attached to these (e.g. pressure, position and surface condition, diameter, etc.) and hence are not applicable, in general, for other regimes and conditions. Hence a general solution of the temperature history valid for all the regimes of boiling has not, so far, been proposed because of the complexities



involved.

The purpose of this thesis is to present an exact solution for the surface temperature of a sphere cooled by boiling which is valid for a wide range of Biot numbers. The term exact is herein used because any degree of accuracy can be achieved in the numerical solution technique. The proposed solution is valid for any range of temperatures as long as the basic assumptions are satisfied (chapter 3). Once the surface temperature is known, the interior temperature can be found by numerical quadrature. With knowledge of the surface temperature, the surface heat flux can be easily calculated. The solution technique is flexible enough to take care of the variations in geometry, if desired. The only pre-condition to this solution is that  $h$  must be known for all temperatures.

The first step in this investigation is the mathematical formulation of the physical problem. The linear partial differential equation for transient heat conduction in spherical coordinates with a temperature dependent heat transfer coefficient is transformed into a nonlinear Volterra integral equation of the second kind for the surface temperature by means of Laplace transformation. Two methods for solving the integral equation are presented. The first method solves the integral equation by successive approximations, while the second method transforms the integral equation into a set of nonlinear first order differential equations. The later method is known as the "Separable Kernel Method". Results are presented for both the methods and compared with each other and also with the experimental results of Stolz, Paschkis et. al. [1].

## II REVIEW OF LITERATURE

### A. Discussion

The transient heat conduction problem connected with quenching presents an extremely nonlinear boundary condition because of the strong dependence of the heat transfer coefficient on the surface temperature. The results of many investigations are available on transient heat conduction problems covering a broad range of nonlinear boundary conditions. But so far, the nonlinear convective boundary condition problem has received little attention.

The present review of literature will consist of two parts. In the first part, investigations concerning boiling heat transfer coefficient will be discussed. It has been mentioned in the introduction that the boiling heat transfer coefficient  $h$  does not have a simple relationship with the surface temperature. But the analytical solution to the present problem is not possible unless  $h$  is known for all temperature. Initially the investigations concerning  $h$  were carried out mainly for metallurgical reasons in quenching but eventually turned out to be of significant importance in the field of heat transfer. In the second part of the review, investigations of transient heat conduction problems with temperature dependent heat transfer coefficients and other kinds of nonlinear boundary conditions will be considered.

A comprehensive study of the heat transfer coefficient in connection with quenching was presented by Stolz, Paschkis et. al. [1]. In their report, Stolz and Paschkis [3], stated the importance of heat transfer coefficient for regulation of the material hardness with the quenching process. By performing a series of quenching

experiments in oil, Stolz, Paschkis et. al., obtained a complete range of heat transfer coefficient data covering all the regimes of boiling [1]. Three different kinds of oil, designated as slow, intermediate and fast and two inch diameter silver spheres were used as quenchents and solids respectively. In the referenced data, the initial temperature of the solid was  $1600^{\circ}$  F and the bulk temperature of the liquid was  $110^{\circ}$  F. From the measured values of the interior temperatures, Stolz obtained the surface temperature of the sphere by a special numerical technique [4]. The method used to obtain the heat transfer coefficient from the surface temperature is described in detail in [1] and [4].

Heinlhofer [5], and later Grossman and Ashimow [6] assumed constant heat transfer coefficient during boiling. However, Stolz, Paschkis et. al. [1] considered the importance of a variable heat transfer coefficient during quenching.

Engel [7], Wever and Rose [8] and Rose [9] performed quenching experiments to compare the cooling rates of silver spheres. Their experimental techniques were later taken up by Stolz, Paschkis et. al. [1], Russel [10] and Yoshida [11, 12, 13] who were also interested in determining heat transfer coefficients for different combinations of solids and liquids. A brief review of their work has already been given in [1] and hence need not be repeated here.

A complete range of heat transfer coefficient data for all the regimes of boiling are also presented by Merte and Clarke [14] and Veers and Florschuetz [15] for two different combinations of solid and liquid. Merte and Clarke obtained their data with a copper sphere - liquid nitrogen system at standard and near zero gravity

using a transient technique. Veers and Florschuetz compared the steady state and transient pool boiling data for a copper sphere - freon 113 system.

Another study on quenching and heat transfer coefficients has been made by Paschkis [16]. Other available papers on quenching [17, 18, 19, 20, 21, 22, 23, 24, 25] mostly deal with metallurgical aspects of quenching.

In this portion of the review, a brief discussion of the past literature, dealing with nonlinear heat conduction is made. A useful comparative study can, therefore, be made between the other method and the present author's method. However, since an extensive discussion of the past literature concerning radiation boundary conditions, has already been made by Crosbie [29], the present discussion will be limited to the pertinent literature which was not discussed by Crosbie.

For convenience, this portion of the review is presented in a tabular form, naming the author(s), the problem statement and the methods of solution. Unless mentioned in the table, all the problems discussed are one dimensional transient heat conduction problems with constant physical properties.

After study of the table, and from the literature survey of Crosbie [29], it can be seen that most of the techniques used for the solution of nonlinear heat conduction problems are different combinations of analytical and numerical ones. Analytical techniques have been adopted to transform the general heat conduction equation (linear or nonlinear) with a set of nonlinear boundary conditions

into a more desired form. Numerical techniques are then employed for the practical solution of the problem. Some of the most common analytical techniques are the heat balance integral method, Biot's variational calculus method and the Laplace transformation method.

Some of the numerical solutions listed in the table are presented in a general form. Gaumer [26] and Gay and Cameron [31] have not discussed the solution of a nonlinear conduction problem, in particular, but have compared the use and applications of different finite difference methods in transient heat conduction problems. A table of comparative studies of five different finite difference techniques is provided in [31] from which a particular method can be selected according to the suitability of the problem. Mason [36] in her numerical solution of a radiating surface has mostly concentrated on showing the advantages of the implicit Runge-Kutta method over the explicit one. However she has not mentioned any particular geometry.

Reference should be made to the investigations of Rosen [41], since among other things, he has also treated the temperature dependent heat transfer coefficient problem. However, he assumed a power law variation of the heat transfer coefficient. Although this assumption is a definite improvement over the assumption of a constant heat transfer coefficient, it is still a long way from the actual case. Thus, his proposed solution for the temperature distribution in a semi-infinite solid with a temperature dependent heat transfer coefficient, cannot be generalized to account for all regimes of boiling.

From this review of the past literature, it can be concluded that besides the work of Rosen [41], not much attention has been given to

nonlinear convective boundary condition problems. Previous work on nonlinear boundary condition problems have mostly centered around radiation boundary conditions. Some exact results for this case, have been reported for the semi-infinite solid, plate, cylinder and sphere. A method is considered exact in the sense that any degree of accuracy can be achieved. In all cases studied, the body was assumed initially at a uniform temperature and free of heat sources. But so far, no exact solution has been proposed for the transient heat conduction problem with nonlinear convective boundary conditions.

## B. Tabular Form

<u>Author(s) Reference No.</u>	<u>Geometry, boundary condition and nature of the problem</u>	<u>Method of solution</u>
Gaumer [26]	slab, cooling or heating by conduction, convection or radiation.	forward, central and backward finite difference; stability of different methods compared.
Ivanov and Salomatorov [27]	one dimensional solid, heat conduction with time dependent heat transfer coefficient.	approximate analytical technique.
Crosbie and Viskanta [28]	one dimensional solids; heating or cooling by radiation	using Laplace transformations the surface temperature expressed in terms of a Volterra integral equation; solved numerically by successive approximations.
Crosbie [29]	one dimensional solids, heated or cooled by convection and/or radiation.	method of solution same as [28]; some approximate methods also proposed.
Winter [30]	semi-infinite solids with parallel walled cavities; cooled by conduction in the interior and radiation at the surface.	numerical solutions; similar calculations performed for the same material without cavities; results of two cases compared.
Gay and Cameron [31]	plate, radiation and adiabatic boundary condition.	five different finite difference methods considered and a comparative study made.

<u>Author(s) Reference No.</u>	<u>Geometry, boundary condition and nature of the problem</u>	<u>Method of solution</u>
Crosbie and Viskanta [32]	plate, heating or cooling by combined convection and radiation.	method same as [28]
Adarkar and Hartstook [33]	semi-infinite solid; heat conduction with time varying radiation boundary condition.	integral method.
Vardi and Lamlich [34]	finite cylinder, steady state heat conduction with radiation boundary condition and with distributed heat source; two dimensional problem.	finite difference; graphical results.
Vadin [35]	infinite slab, simultaneous convection and radiation at the boundary.	integral equation of temperature distribu- tion solved by iter- ation method assuming a cubic temperature profile.
Crosbie and Viskanta [36]	one dimensional solid, heated or cooled by radiation.	kernel of the trans- formed Volterra integral equation approximated by a separable kernel; resulting nonlinear differential equation solved numerically; solution not practical for small time.
Mason [37]	slab; radiating boundary condition.	implicit Runge-Kutta method which is uncon- ditionally stable and much faster than the explicit method.



<u>Author(s) Reference No.</u>	<u>Geometry, boundary condition and nature of the problem</u>	<u>Method of solution</u>
Abrams [38]	sphere, cooled by radiation.	method same as [28].
Ayers [39]	cylinder; cooled by radiation	finite difference; results in graphical forms for a wide range of parameters.
Ayers [40]	sphere; cooled by radiation	same as [39].
Rosen [41]	semi-infinite solid; heated or cooled by convection and/or radiation at the surface; variable thermophysical pro- perties.	heat balance integral method; resulting ordinary differential equation solved numerically.
Graham [42]	one dimensional solids; simultaneous convection and radiation.	by using Laplace and Z transformations on the governing heat conduction equation, a discrete time system of equations is obtain- ed for digital computer solution; results in good agreement with [28].
Vujanovic [43]	rod and slab; both linear and nonlinear boundary conditions are treated.	variational technique; solution expressed in analytic closed form; results are in good agreement with known solutions.

### III MATHEMATICAL FORMULATION OF THE PROBLEM

This investigation is concerned with the transient surface temperature of a sphere, initially heated to a uniform temperature and then suddenly placed in a cool liquid. The initial temperature difference between the sphere and the liquid is large enough such that film, transition and nucleate boiling and free convection occur at the surface of the sphere during cooling. The heat transfer coefficient under this circumstance is a strong function of the surface temperature and hence the governing boundary condition becomes extremely nonlinear.

Following are the basic assumptions made in the investigation:

1. The heat conduction is one dimensional.
2. The sphere is isotropic, homogenous and opaque to thermal radiation.
3. The physical properties (  $\rho$ ,  $C_p$  and  $k$  ) are independent of temperature.
4. The bath temperature remains constant.
5. The heat transfer coefficient  $h$  is independent of the diameter of the sphere.

Special mention should be made about the last assumption. The values of  $h$  used in this analysis were determined for a 2 inch diameter silver sphere ( $Bi \doteq .50$ ) by Stolz et. al. [1]. In the experiments performed by Stolz et. al., the surface temperature was measured and then a lumped parameter technique was applied to calculate  $h$ . Hence, the analytical solution for the temperature of the sphere becomes trivial, since the surface temperature was already measured to determine  $h$ . However, it is not always convenient to make laboratory

measurements of the surface temperatures for a wide range of physical situations. Hence, with the knowledge of  $h$  for one particular diameter of the sphere and with the assumption No. 5, the surface temperature for a wide range of diameters can be determined numerically. Also when the dependency of  $h$  on the diameter of the sphere can no longer be ignored, the technique of Reference [1] can be employed to determine  $h$  by employing a hollow sphere so that the lumped parameter approximation can be applied (essentially true for a small  $Bi$ ). With these known values of  $h$ , the solution technique can then be suitably applied to determine the surface temperature of a solid sphere of the same external diameter as the hollow one.

The differential equation governing the transient temperature distribution, therefore, is

$$\frac{\partial T}{\partial t_1} = \frac{\alpha}{r_1^2} \frac{\partial}{\partial r_1} \left( r_1^2 \frac{\partial T}{\partial r_1} \right) \quad (1)$$

The initial and boundary conditions are

$$T(r_1, 0) = T_i \quad (2a)$$

$$-k \left. \frac{\partial T}{\partial r_1} \right|_{r_1 = R} = h(T_s) [T_s - T_c] \quad (2b)$$

$$\left. \frac{\partial T}{\partial r_1} \right|_{r_1 = 0} = 0 \quad (2c)$$

To simplify the analysis, the basic equation (1) and the initial and boundary conditions (2a, 2b, and 2c) are expressed in dimensionless forms by the following substitutions:

$$t = \frac{\alpha t_1}{R^2}, \quad r = \frac{r_1}{R} \quad \text{and} \quad u(r, t) = \frac{T(r, t)}{T_i}$$

Thus, we obtain

$$\frac{\partial^2 u}{\partial r^2} + \frac{2}{r} \frac{\partial u}{\partial r} = \frac{\partial u}{\partial t} \quad (3)$$

and

$$u(r, 0) = 1 \quad (4a)$$

$$\left. \frac{\partial u}{\partial r} \right|_{r=1} = -g [u_s(t)] \quad (4b)$$

$$\left. \frac{\partial u}{\partial r} \right|_{r=0} = 0 \quad (4c)$$

In equation (4b)

$$g [u_s(t)] = Bi \frac{h}{h_{\max}} (u_s - \theta_c) \quad (4d)$$

where  $Bi = \frac{h_{\max} R}{k}$

The solution of the above set of equations (3), (4a), (4b), (4c), and (4d) remains incomplete unless the values of  $h$  are explicitly known for all the surface temperatures. In this regard, Reference [1] was consulted.

Figure (3) in Reference [1] represents the behavior of  $h$  with surface temperature for a particular quenching experiment using oil as a quenchant. The bulk temperature of the quenchant was  $110^\circ \text{F}$  and the initial temperature of the spherical sample was  $1600^\circ \text{F}$ .  $h$  is represented in the semilogarithmic scale in Figure (3) from Reference [1] and thus the interpolation of  $h$  becomes difficult.

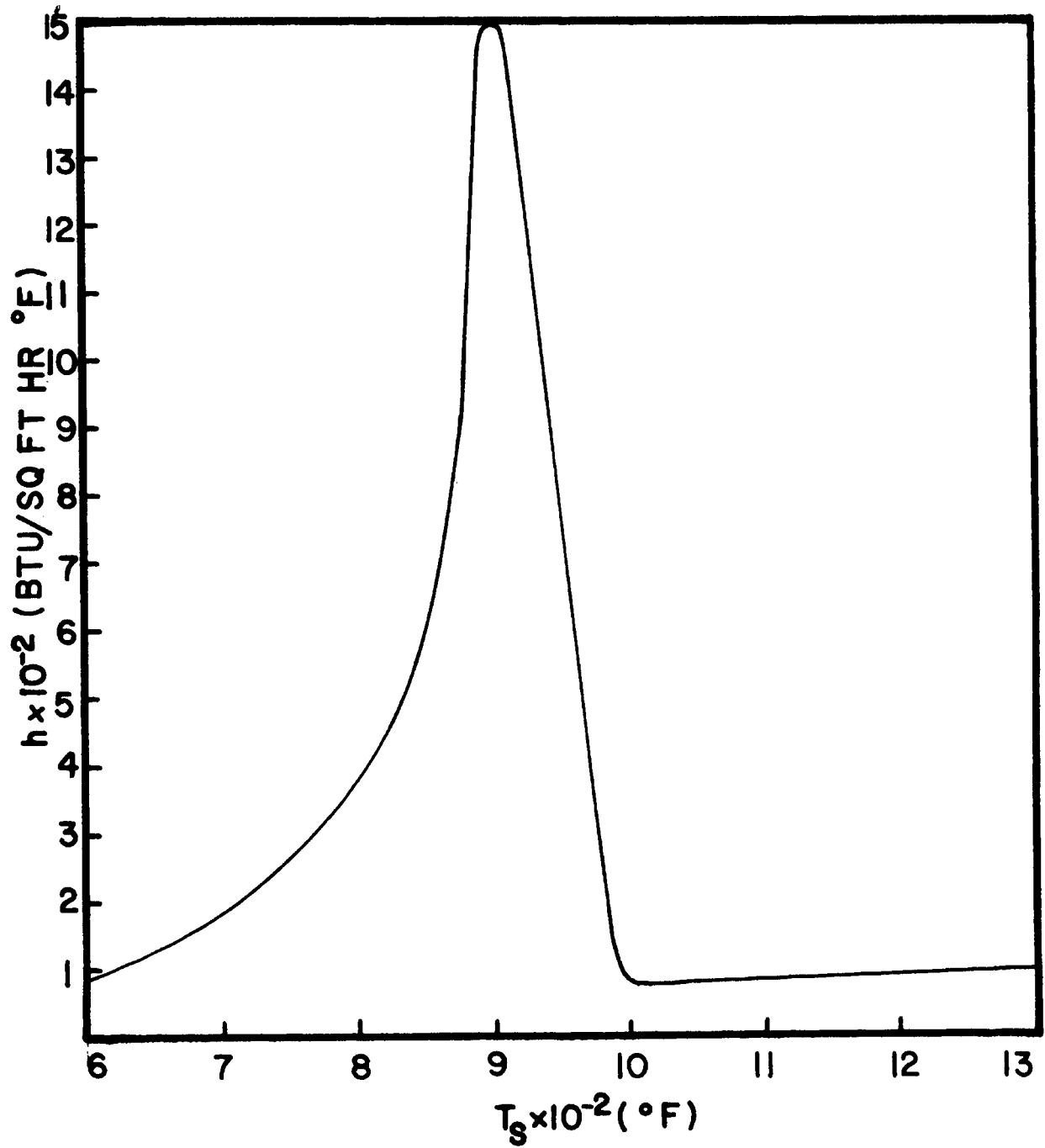


Fig. 3 Variation of Heat Transfer Coefficient with Surface Temperature as used in this analysis.

However, several data points were selected carefully from this graph. These points were tested by a suitable interpolation routine. Testing was done numerically on a digital computer and minor adjustments in the input data were made until a smooth curve was obtained through these points. Figure (3) represents the final form of the  $h - T_g$  relationship used in the solution.

The numerical program had to be run a number of times because of the abrupt behavior of  $h$  where a change from one boiling regime to the next takes place. In these regions, as can be seen from Figures (1a) and (3),  $h$  is very sensitive to minor changes in  $T_g$ . The interpolating routine failed to interpolate the desired value correctly unless more data points were added to these regions. The nature of this particular interpolating routine is such that the routine picks up three input values on both sides of the desired point and computes the value based on the information provided by these six points. Hence, if the input points on either side are quite far apart, the interpolation method fails to pick up the nature of the curve correctly. After several trial and error runs, a total of 136 points were used and smooth curve of  $h$  versus  $T_g$  was obtained.

Following the procedure of Crosbie [29], the partial differential equation (3) along with the initial and boundary conditions (4a), (4b) and (4c) is transformed into a single nonlinear Volterra integral equation of the second kind by the use of the Laplace transformation with respect to time  $t$  and the application of the convolution theorem. The Laplace transformation of equations (3), (4b) and (4c) produces the following ordinary differential equation:

$$\frac{d^2 \bar{u}}{d r^2} + \frac{2}{r} \frac{d \bar{u}}{d r} - s \bar{u} = -1 \quad (5)$$

with the transformed boundary conditions

$$\left. \frac{d \bar{u}}{d r} \right|_{r=0} = 0 \quad (6a)$$

$$\left. \frac{d \bar{u}}{d r} \right|_{r=1} = -\bar{g} [u_s] \quad (6b)$$

The solution to the above set of equations is

$$\bar{u}(r,s) = \frac{1}{s} - \frac{1}{r} [\bar{g}(u_s) \cdot \bar{F}(r,s)] \quad (7)$$

where the function  $\bar{F}(r,s)$  is expressed as, Reference [38]

$$\bar{F}(r,s) = \frac{\sinh(\sqrt{s} r)}{\sqrt{s} \cosh \sqrt{s} - \sinh \sqrt{s}} \quad (8)$$

The inverse of equation (7) is then symbolically given by

$$u(r,t) = 1 - \frac{1}{r} \mathcal{L}^{-1} [g(u_s) \cdot \bar{F}(r,s)] \quad (9)$$

The inverse of the right hand side of the above equation follows immediately with the help of the convolution theorem. The convolution property is stated as follows:

$$\overline{uv} = \overline{u * v} = \int_0^t u(\tau) v(t-\tau) d\tau$$

Thus, with the help of the convolution theorem

$$\mathcal{L}^{-1} [\bar{g}(u_s) \cdot \bar{F}(r,s)] = \int_0^t g[u_s(\tau)] F(r,t-\tau) d\tau \quad (10)$$

Substitution of equation (10) into equation (9) yields

$$u(r,t) = 1 - \frac{1}{r} \int_0^t g[u_s(\tau)] F(r,t-\tau) d\tau \quad (11)$$

Equation (11) is the integral equation of the problem. However, it is not yet usable as a solution since the unknown function  $g [u_s(t)]$  which was defined earlier appears under the integral sign. Hence  $F(r,t)$  has to be explicitly found by using the inversion theorem for the Laplace Transformations.

$$\begin{aligned}
 F(r,t) &= \mathcal{L}^{-1} [ \bar{F}(r,s) ] = \frac{1}{2\pi i} \int_{c-i\infty}^{c+i\infty} \bar{F}(x,s) \exp(st) dt \\
 &= \frac{1}{2\pi i} \int_{c-i\infty}^{c+i\infty} \frac{\sinh(\sqrt{z}r) \exp(zt)}{\sqrt{z} \cosh \sqrt{z} - \sinh \sqrt{z}} dz
 \end{aligned} \tag{12}$$

where  $c$  is a positive constant in the complex plane lying to the right of the singularities of the integrand. Equation (12) is integrated by means of contour integration and the Cauchy Residue theorem with the result:

$$F(r,t) = 3r + 2 \sum_{k=1}^{\infty} \frac{\sin \lambda_k r}{\sin \lambda_k} \exp(-\lambda_k^2 t) \tag{13}$$

where the eigenvalues  $\lambda_k$  are defined by  $\tan \lambda_k = \lambda_k$ , the  $\lambda = 0$  case excluded. Substitution of (13) into (11) yields

$$\begin{aligned}
 u(r,t) = 1 - \int_0^t g [ u_s(\tau) ] \left[ 3 + 2 \sum_{k=1}^{\infty} \frac{\sin \lambda_k r}{r \sin \lambda_k} \right. \\
 \left. \exp(-\lambda_k^2 (t - \tau)) \right] d\tau
 \end{aligned} \tag{14}$$

Equation (14) implies that the surface temperature  $u_s$  must be known as a function of time before any interior temperature can be found. The integral equation for the surface temperature is obtained simply by putting  $r$  equal to unity in equation (14):



$$u_s(t) = 1 - \int_0^t g[u_s(\tau)] \left[ 3 + 2 \sum_{k=1}^{\infty} \exp(-\lambda_k^2 (t - \tau)) \right] d\tau \quad (15)$$

Thus, the problem of transient cooldown of a sphere with a uniform initial temperature distribution and subject to nonlinear convective boundary conditions can be reduced to the solution of a single nonlinear Volterra integral equation of the second kind for the surface temperature, equation (15). Once the surface temperature  $u_s(t)$  is known from equation (15), the interior temperature at any position and time can be determined by substituting the value of  $u_s(t)$  in equation (14) and then by subsequent integration for any known time.

IV SOLUTIONS OF THE INTEGRAL EQUATION

(A) Modified Successive Approximation Method

The integral equation (15) is solved by a modified successive approximation method. The use of the term 'modified' seems justified here since, as is described later, the present method breaks the total time into a convenient number of intervals and a successive approximation is applied over each of these intervals. But in the standard method of successive approximations an approximation is applied over the entire time period.

Equation (15) can be rewritten with the substitution  $Y(t) = u_g(t)$  (for convenience)

$$Y(t) = 1 - \int_0^t g [ Y(\tau) ] \left[ 3 + 2 \sum_{k=1}^{\infty} \exp(-\lambda_k^2(t-\tau)) \right] d\tau \quad (16)$$

$$(t \geq 0)$$

To obtain the solution of the above equation, the entire time range for which the solution is desired, is divided into a suitable number of intervals. For the first time interval,  $0 \leq t \leq t_1$ , an approximation for the unknown temperature is made. With this initial value, successive approximations of the temperature are made for the first time interval using equation (16). Thus, the  $(n+1)$ th approximation is given by

$$Y_{n+1}(t) = 1 - \int_0^t g [ Y_n(\tau) ] \left[ 3 + 2 \sum_{k=1}^{\infty} \exp(-\lambda_k^2(t-\tau)) \right] d\tau \quad (17)$$

$$(0 \leq t \leq t_1)$$

Each of the following approximations is improved from the preceding one until the difference between the last two approximations becomes less than a predetermined error criterion.

For the second time interval, the integral equation (16) is broken into two parts, the first being the time interval for which the solutions are already known from (17). This results in:

$$\begin{aligned}
 Y_{n+1}(t) = & 1 - \int_0^{t_1} g[Y(T)] \left[ 3 + 2 \sum_{k=1}^{\infty} \exp(-\lambda_k^2(t-T)) \right] dT \\
 & - \int_{t_1}^t g[Y_n(T)] \left[ 3 + 2 \sum_{k=1}^{\infty} \exp(-\lambda_k^2(t-T)) \right] dT \\
 & (t_1 \leq t \leq t_2)
 \end{aligned} \tag{18}$$

The second term of the above equation is completely known for all time  $t$ . Hence, an approximation for the unknown temperature is made for the time interval  $t_1 \leq t \leq t_2$ . Again by the method of successive approximations, each of the following approximations is improved in equation (18), until the difference between the last two approximations meets the error criterion.

In general, for  $m$  time intervals, equation (18) takes the form

$$\begin{aligned}
 Y_{n+1}(t) = & 1 - \int_0^{t_m} g[Y(T)] \left[ 3 + 2 \sum_{k=1}^{\infty} \exp(-\lambda_k^2(t-T)) \right] dT \\
 & - \int_{t_m}^t g[Y_n(T)] \left[ 3 + 2 \sum_{k=1}^{\infty} \exp(-\lambda_k^2(t-T)) \right] dT \\
 & (t_m \leq t \leq t_{m+1})
 \end{aligned} \tag{19}$$

This process is continued until the surface temperature for all desired time is known.

Although the process may seem theoretically simple, an analytical solution of equation (19) is, in general, highly impractical. For example, if we start with a simple initial approximation  $Y_0 = 1$ , assuming  $\theta_c = 0$ , the dimensionless flux term in equation (17) is given by:

$$g[Y_0(T)] = Bi \frac{h(1)}{h_{\max}} [1 - 0] = Bi H(Y_0) \quad (20)$$

denoting  $h(Y_n)/h_{\max}$  by  $H(Y_n)$ .

Next the approximation  $Y_1$  is, therefore, given by:

$$Y_1 = 1 - \int_0^t Bi H(1) \left[ 3 + 2 \sum_{k=1}^{\infty} \exp(-\lambda_k^2(t-T)) \right] dT \quad (21)$$

$(0 \leq t \leq t_1)$

It is evident from the above equation that determination of  $Y_1$  involves the calculation of an infinite series and the values of  $H(1)$ .

Determination of the next approximation  $Y_2$ , as can be seen from equation (18), will then depend upon a new value of  $H(Y_1)$  and the substitution of new limits on the infinite series. Thus, the calculations of subsequent approximations becomes too complicated to solve manually even with a simple starting value. Hence the use of a numerical technique, in this case, becomes an obvious necessity.

Since a suitable numerical technique makes the use of an analytical solution practical, a brief description of the numerical procedure should be given. Each time interval is subdivided equally into as many points as necessary so that a curve can be fitted for a numerical

interpolation formula to produce an error less than that desired of the surface temperature. This interpolation formula is necessary for the use of the Gaussian Quadrature formula [51] for evaluation of the integrals of equation (18). In this method, the ordinary Gaussian integration formula is used to evaluate

$$\int_0^t g [Y(T)] \left[ 3 + 2 \sum_{k=1}^{\infty} \exp(-\lambda_k^2 (t-T)) \right] dT$$

and a modified Gaussian formula is used to evaluate

$$\int_{t_m}^t g [Y_m(T)] \left[ 3 + 2 \sum_{k=1}^{\infty} \exp(-\lambda_k^2 (t-T)) \right] dT$$

The two forms of Gaussian integration formulas are as follows:

$$\int_a^b f(y) dy = \frac{b-a}{2} \sum_{i=1}^{\infty} w_i f(y_i), \quad y_i = \frac{b-a}{2} x_i + \left(\frac{b+a}{2}\right) \quad (22)$$

and

$$\int_a^b f(y) (b-y)^{-\frac{1}{2}} dy = 2 \sqrt{b-a} \sum_{i=1}^{\infty} w_i^{(2n)} f(y_i), \quad (23)$$

$$\text{where } y_i = a + (b-a)(1-x_i)^2$$

The Gaussian weights  $w_i$  and  $w_i^{(2n)}$  and the abscissa  $x_i$  are defined in Reference [51].

One interesting thing to note is that equation (23) eliminates the singularity of the integral, Reference [52, 53]. The efficiency of the Gaussian quadrature method is much higher than other standard numerical integration techniques [52, 53].

The basic difference between the numerical and analytical approach is that the method of successive approximations is carried out point by point instead of integrating over the entire time interval.

The initial guess in the method of successive approximations is of

vital importance for a fast convergence of the method to the exact solution. This is particularly true for the present problem where the heat transfer coefficient changes drastically with a small change of time in certain regions of cooling as can be seen from the  $h$  versus  $T_s$  curve, Figure (3). The rate of change of temperature is very high in these regions, compared to the other regimes of cooling. Hence, unless the initial approximation of the temperature at these points of sudden changes is sufficiently close to the exact solution, much of the computer time will be lost in attaining a suitable convergence. Thus, the method for obtaining a suitable initial value is of particular interest.

The method of intersection as used by Crosbie [29], was initially employed for determining the initial values. But it was found that for a Biot number larger than 1.0, this method failed to produce a convergence within a preset number of iterations. Obviously the guess was too far away from the actual value to produce a suitable convergence. Hence a method for obtaining a closer approximation to the actual case was sought.

The infinite thermal conductivity solutions are found to be close approximations to the actual cases and hence are used as the initial guesses in the present problem. This particular method of solutions has been discussed in detail under the heading of 'Separable Kernel Method' in the following section and hence need not be repeated here. Strictly speaking, infinite thermal conductivity solutions used as the initial guesses differ from the standard approach. The total time period, as has been mentioned previously, is broken into different time intervals. Initial guesses for all but one point

in any time interval are determined exactly in the same manner as that of standard infinite thermal conductivity solutions. Only the calculation of the first point in any subsequent interval is based on the exact value of the last point of the preceding interval.

Mathematically this can be shown as

$$dY_1 / dt = -3g(Y_1) \qquad t_m \leq t \leq t_{m+1}$$

where  $Y_1(t_m) = Y(t_m)$

$Y(t_m)$  represents the exact value of the last point in the preceding time interval,  $t_{m-1} \leq t \leq t_m$ .

As illustrated in References [54] and [55] and as can be seen from Figure (4), the ideal solution, in which infinite thermal conductivity was assumed, closely follows the exact solution for small time except at points of sharp changes in temperature. For large time, there is practically no deviation from the exact solution. Hence only at the critical points of sharp changes, initial guesses are comparatively far away from the exact solutions and therefore, require more iterations for convergence.

The particular method of solution for the cooling of a sphere with nonlinear convective boundary conditions can also be applied to other geometries. It can also take into account the effect of non-uniform initial temperature, heat sources and some other forms of nonlinear boundary conditions. The major difference in the integral equations between the sphere and other geometries is the kernel  $F(x,t)$ . The kernel for the surface temperature  $f(t-T)$  is obtained by replacing  $x$  by 0 for a semi-infinite solid and by 1 for other

geometries in  $F(x,t)$ .

For a semi-infinite solid:

$$f(t-T) = [\pi(t-T)]^{-\frac{1}{2}} \quad (24)$$

For a plate:

$$f(t-T) = 1 + 2 \sum_{k=1}^{\infty} \exp(-\lambda_k^2(t-T)) \quad (25)$$

with eigenvalues  $\sin \lambda_k = 0$  or  $\lambda_k = k \pi$ .

For a Cylinder:

$$f(t-T) = 2 + 2 \sum_{k=1}^{\infty} \exp(-\lambda_k^2(t-T)) \quad (26)$$

with the eigenvalues given by  $J_1(\lambda_k) = 0$ . Physically a plate, cylinder and sphere behave like a semi-infinite solid over a small time period.



## (B) Separable Kernel Method

An alternate method for solution of the Volterra integral equation which determines the surface temperature of the sphere is described in this section. The method is based on approximating the kernel by a separable kernel. The method is exact except for very small time. The natural appeal of this method is its ease of application and the independence of each approximation.

The integral equation for the surface temperature, ( $Y(t) = u_s(t)$ ) of the sphere is as follows:

$$Y(t) = 1 - \int_0^t g [ Y ( T ) ] f(t- T) d T$$

where the kernel  $f(t- T)$  is  $3 + 2 \sum_{k=1}^{\infty} \exp (- \lambda_k^2 (t- T))$ .

The zeroth order approximation is obtained by neglecting all the terms of the infinite series of the kernel. The first order approximation is obtained by including the first term of the series, the second order approximation by including the second term, the third order approximation by taking up to the third term and so on depending upon the degree of accuracy required. Evidently the greater the number of terms, the better will be the accuracy since the kernel is represented more accurately.

The zeroth order approximation gives the following integral equation:

$$Y(t) = 1 - 3 \int_0^t g [ Y( T ) ] d T \quad (27)$$

Differentiating the above with respect to time transforms the above equation into a first order nonlinear differential equation:

$$\frac{dY}{dt} = -3g[Y] \quad (28)$$

with the initial condition  $Y(0) = 1$ .

The ordinary differential equation (28) describes the temperature history of the sphere with infinite thermal conductivity. The solution of equation (28) is the large time solution of equation (16) since the infinite series of the kernel tends to zero as time approaches infinity.

$$\lim_{t \rightarrow \infty} \exp[-\lambda_k^2 (t-T)] = 0.$$

The first order approximation as explained, can be obtained by replacing the kernel by  $3 + 2 \exp[-\lambda_1^2 (t-T)]$ .

The resulting integral equation is:

$$Y(t) = 1 - 3 \int_0^t g[Y(T)] dT - 2 \exp(-\lambda_1^2 t) \int_0^t \exp(\lambda_1^2 T) g[Y(T)] dT \quad (29)$$

This equation can be rewritten as

$$Y(t) = Y_0(t) + Y_1(t) \quad (30)$$

$$\text{where } Y_0(t) = 1 - 3 \int_0^t g[Y(T)] dT \quad (31)$$

$$\text{and } Y_1(t) = -2 \exp(-\lambda_1^2 t) \int_0^t \exp(\lambda_1^2 T) g[Y(T)] dT. \quad (32)$$

Differentiation of equations (31) and (32) with respect to time yields two first order linear differential equations of the following forms:

$$\frac{dY_0}{dt} = -3 g[Y(t)] \quad (33)$$

$$\frac{dY_1}{dt} = -2 g[Y(t)] - \lambda_1^2 Y_1(t) \tag{34}$$

The two equations (33) and (34) are provided with two initial conditions

$$Y_0(0) = 1$$

and (35)

$$Y_1(0) = 0$$

These two first order linear differential equations can be easily solved by numerical means.

In general the Mth order approximation can be found by replacing the infinite series by

$$\sum_{k=1}^M \exp[-\lambda_k^2(t-T)]$$

and, therefore, the resulting integral equation is

$$Y(t) = 1 - 3 \int_0^t g[Y(T)] dT - 2 \sum_{k=1}^M \int_0^t \exp[-\lambda_k^2(t-T)] g[Y(T)] dT \tag{36}$$

As before, Y(t) can be assumed to be composed of M + 1 parts as follows:

$$Y(t) = Y_0(t) + Y_1(t) + Y_2(t) + \dots + Y_M(t) \tag{37}$$

where  $Y_0(t) = 1 - 3 \int_0^t g[Y(T)] dT$

$$Y_1(t) = -2 \exp(-\lambda_1^2 t) \int_0^t \exp(\lambda_1^2 T) g[Y(T)] dT$$

$$Y_2(t) = -2 \exp(-\lambda_2^2 t) \int_0^t \exp(\lambda_2^2 T) g[Y(T)] dT$$

$$\dots \tag{38}$$

$$Y_M(t) = -2 \exp(-\lambda_M^2 t) \int_0^t \exp(\lambda_M^2 \tau) g[Y(\tau)] d\tau$$

Differentiation of the above set of equations yields

$$\frac{dY_0}{dt} = -3 g[Y(t)]$$

$$\frac{dY_1}{dt} = -2g[Y(t)] - \lambda_1^2 Y_1(t)$$

$$\begin{array}{l} - \quad - \quad - \quad - \quad - \quad - \quad - \quad - \quad - \quad - \quad - \quad - \quad - \quad - \quad - \quad - \\ - \quad - \quad - \quad - \quad - \quad - \quad - \quad - \quad - \quad - \quad - \quad - \quad - \quad - \quad - \end{array} \quad (39)$$

$$\begin{aligned} \frac{dY_M}{dt} &= -2g[Y(t)] - 2(-\lambda_M^2) \exp(-\lambda_M^2 t) \\ &\quad \int_0^t \exp(\lambda_M^2 \tau) g[Y(\tau)] d\tau \\ &= -2g[Y(t)] - \lambda_M^2 Y_M(t) \end{aligned}$$

For these  $M + 1$  nonlinear differential equations (39), the initial conditions are

$$Y_0(0) = 1 \text{ and } Y_1(0) = Y_2(0) = Y_3(0) = \dots = Y_M(0) = 0 \quad (40)$$

which makes

$$Y(0) = Y_0(0) + Y_1(0) + Y_2(0) + \dots + Y_M(0) = 1$$

Therefore, these  $M + 1$  linear, interlinked, first order differential equations with the given initial conditions are easily solvable with the use of a digital computer. There are some standard subroutine packages in the computer built-in library which can be conveniently used. This author has used subroutine RKGS from System/360 Scientific Subroutine Package, (360 A - CM - 03X) version III of IBM Fortran language. The zeroth order solution was also computed by the use

of a standard fourth order Runge-Kutta method and the Adams Moulton corrector predictor method.

The separable kernel method was also discussed and presented by Crosbie and Viskanta [36] but their final form of the differential equations was different from the one presented here. The basic approach of replacing the infinite series of the kernel  $f(t-T)$  by a finite number of terms is the same. In this presentation, the temperature  $Y(t)$  in equation (37) is broken up in  $(M + 1)$  different parts. In Reference [36],  $Y(t)$  was differentiated successively  $(M + 1)$  times resulting in  $(M + 1)$  integrodifferential equations of different orders. By the simultaneous elimination of the integral terms from these equations an  $(M + 1)$ th order differential was obtained. The  $M + 1$  initial conditions were also presented to solve the differential equation.

The present method has some advantages over Crosbie and Viskanta's. In the present formulation, no simultaneous elimination of integral terms is necessary. The set of  $(M + 1)$  nonlinear first order equations, equations (39), is obtained by simple substitutions. The differential equation obtained in Reference [36], contains the derivatives of the unknown term  $g$  on the right hand side of the equation. ' $g$ ' is a function of the unknown temperature  $Y$  and hence the presence of different order derivatives of  $g$  makes the solution complicated. In the present formulation, equations (39) do not contain any derivative term of  $g$ . Also the initial conditions of the present method are much simpler to work with than in Reference [36]. Thus, the present method is an improvement over Crosbie and Viskanta's separable kernel method.

## (C) Modified Separable Kernel Method

A modified version of the separable kernel method is presented in this section. In the preceding section  $Y(t)$  was represented by a summation of  $M + 1$  terms of equal weights, equation (37). But here  $Y(t)$  has been assumed to be of the following form:

$$Y(t) = Y_0(t) + Y_1(t) + Y_2(t) + \dots + \epsilon_M Y_M(t) \quad (41)$$

In the above equation  $\epsilon_M$  is a weighted coefficient for the last term and can be determined as follows.

The kernel  $f(t)$  for the sphere from equation (13) is given by:

$$f(t) = 3 + 2 \sum_{k=1}^{\infty} \exp(-\lambda_k^2 t) \quad (42)$$

$$\text{or } f(t) - 3 = 2 \sum_{k=1}^{\infty} \exp(-\lambda_k^2 t) \quad (43)$$

The infinite series in the above equation can be represented by a finite number of terms with a weighted coefficient in the last term.

$$f_M(t) - 3 = 2 \exp(-\lambda_1^2 t) + 2 \exp(-\lambda_2^2 t) + 2 \exp(-\lambda_3^2 t) + \dots + 2 \epsilon_M \exp(-\lambda_M^2 t) \quad (44)$$

If both sides of equation (43) are integrated from 0 to  $\infty$  with respect to  $t$ , the expression becomes

$$\begin{aligned} \int_0^{\infty} [f(t) - 3] dt &= 2 \sum_{k=1}^{\infty} \int_0^{\infty} \exp(-\lambda_k^2 t) dt \\ &= 2 \sum_{k=1}^{\infty} \frac{1}{\lambda_k^2} \end{aligned} \quad (45)$$

By referring [52] and [53], the infinite series in equation (45) is calculated and found to be

$$\sum_{k=1}^{\infty} \frac{1}{\lambda_k^2} = \frac{1}{10} \quad (46)$$

Therefore, from equations (45) and (46)

$$\int_0^{\infty} [f(t)-3] dt = 2 \sum_{k=1}^{\infty} \frac{1}{\lambda_k^2} = \frac{2}{10} \quad (47)$$

Integration of equation (44) from 0 to  $\infty$  with respect to  $t$  yields

$$\begin{aligned} \int_0^{\infty} [f_M(t)-3] dt &= 2 \sum_{k=1}^{M-1} \left[ \frac{\exp(-\lambda_k^2 t)}{\lambda_k^2} \right]_0^{\infty} + \left[ \frac{2 \epsilon_M \exp(-\lambda_M^2 t)}{\lambda_M^2} \right]_0^{\infty} \\ &= 2 \sum_{k=1}^{M-1} \frac{1}{\lambda_k^2} + \frac{2 \epsilon_M}{\lambda_M^2} \end{aligned} \quad (48)$$

Since equation (43) is approximately represented by equation (44), they are assumed to be equal. Therefore, by equating the right hand sides of equations (47) and (48), we get

$$\begin{aligned} 2 \sum_{k=1}^{M-1} \frac{1}{\lambda_k^2} + \frac{2 \epsilon_M}{\lambda_M^2} &= \frac{2}{10} \\ \text{or } \epsilon_M &= \left[ \frac{1}{10} - \sum_{k=1}^{M-1} \frac{1}{\lambda_k^2} \right] \lambda_M^2 \end{aligned} \quad (49)$$

Hence, equation (49) determines the value of the weighted coefficient in terms of the known eigenvalues, to be used in equation (41). The rest of this proposed solution is exactly similar to that of the preceding section. The form of the derivatives of different terms, equation (39), and the initial conditions, equation (40), remain the same in this method also. The only difference between the methods presented in section (b) and in the present section lies in the mode

of presentation of equations (37) and (41).

The efficiency of the present solution is much higher than that obtained with the ordinary separable kernel method. It has been found that, after the computation of a few values of  $Y(t)$ , all the terms except the first two or three in equation (40), rapidly go to zero. Thus, the effect of additional terms beyond the first two or three, becomes almost nil in the following computations. Hence, the expected improvement by the representation of the kernel with a larger number of terms is not efficiently achieved in the ordinary separable kernel method. But the addition of a weighted coefficient in equation (44) in the modified, largely improves the effect of all the terms up to the last one in the computations of  $Y(t)$ . Proper participation of all the terms up to any desired value of  $Y(t)$  is thus assured in equation (44). The proposed solution requires fewer terms to represent the kernel  $f(t)$  and still to achieve the same amount of accuracy as the ordinary separable kernel method. The increase in efficiency in the modified technique is, therefore, obvious.



## V RESULTS

An inspection of equation (15) reveals that the dimensionless surface temperature  $Y(t)$  is a function of heat flux  $g$  but which in turn is a function of the surface temperature and the heat transfer coefficient. As has been mentioned in Chapter 3, the heat transfer coefficient data for the different surface temperatures used in this study was taken from Reference [1]. The values of  $h$  were based on the quenching of a two inch diameter silver sphere in oil at a constant temperature of  $110^{\circ}$  F as used in the experiment by Stolz et. al. [1]. Hence  $h$  and in turn  $g$  are expected to be different for a different oil temperature. But it has been found by Stolz et. al. [1] that there is virtually no change in the values of  $h$  with the change in the oil temperature as long as the oil temperature remains within the region of sub-cooled boiling, (less than  $600^{\circ}$ F for the kind of oil used in their experiment). Hence the values of  $h$  with oil as quenchant can be considered to be independent of the oil temperature for sub-cooled boiling. With these values of  $h$ , results for surface temperature have been obtained in this study, for four different Biot numbers (i.e. four different size spheres). Once the surface temperature  $u_s$  has been found from equation (15), the interior temperature at any time can be found by the substitution of  $u_s$  in equation (14) and subsequent integration for any known time. With the knowledge of heat transfer coefficients at different surface temperatures, heat fluxes at the boundary have been calculated (described later in this chapter).

Surface temperature versus time curves for Biot numbers of

0.50, 1.0, 5.0 and 10.0 have been plotted in Figure (4), on the same scale. The results corresponding to  $Bi = 0.50$  are of particular interest since experimental results for this case are available, Reference [1]. Strictly speaking, based on the available data for  $k$  at  $68^\circ F$ ,  $Bi$  for the case of Reference [1] turns out to be 0.54 which is 8% higher than 0.50. But it is to be noted that the value of  $k$  for silver changes considerably with temperature (237 Btu/hr. ft  $^\circ F$  at  $32^\circ F$  to 208 Btu/hr. ft  $^\circ F$  at  $752^\circ F$ ). Also the value of  $h_{max}$  used in the calculation of  $Bi = h_{max} R / k$  was read from a semi-logarithmic graph. Hence considering the errors involved, the value of  $Bi = 0.50$  has been accepted as a close approximation for the experimental results in Reference [1]. The values calculated in this study compare favorably with those of Stolz et. al. [1].

In Figure (4), the infinite thermal conductivity solutions (i.e. separable kernel method with one equation) are also presented for all four Biot numbers. The infinite thermal conductivity solutions are shifted along the time scale a distance which is inversely proportional to the ratios of the Biot numbers. This shift can be explained from the mathematical expression obtained with the infinite thermal conductivity assumption.

From equation (31)

$$dY/dt = -3 Bi h/h_{max} (Y - \theta_c) \quad (50)$$

With the substitution of  $t^* = Bi t$ , equation (50) takes the form

$$dY/dt^* = -3 h/h_{max} (Y - \theta_c) \quad (51)$$

It is evident from the above equation that the solution for  $Y$  in terms of  $t^*$  is independent of  $Bi$ . Thus for all values of  $Bi$  there

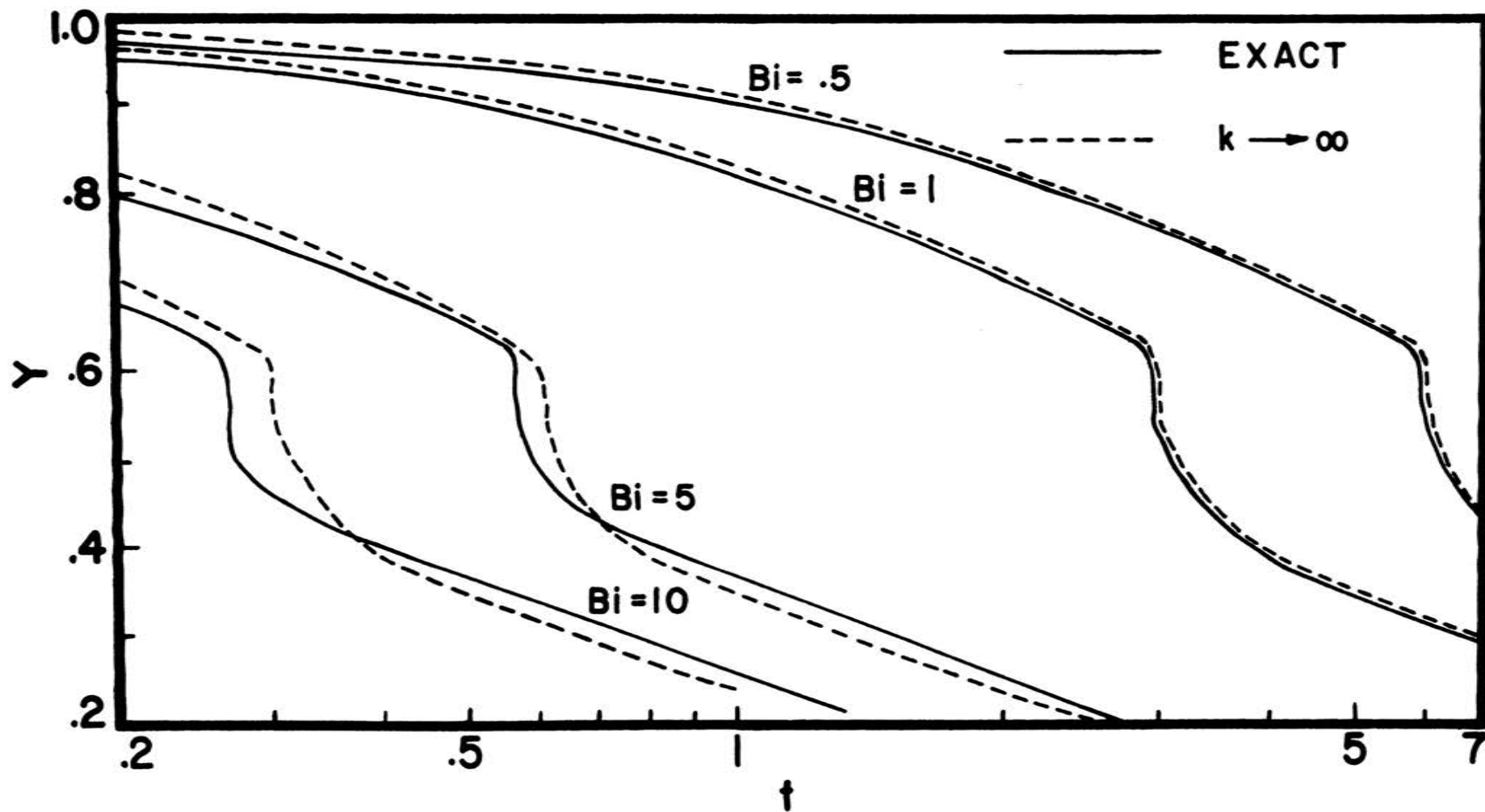


Fig. 4 Surface Temperature Distribution during the Cooling of a Sphere for both Infinite Thermal Conductivity and Exact Solutions for Different Biot Numbers ( $Bi = .5, 1, 5$  and  $10$ ).

is just one solution for  $Y$  in terms of  $t^*$ . Comparison of the solutions for  $Bi = 5.0, 10.0$  and the solution of equation (51) are graphically shown in Figure (5).  $t^*$  is the product of  $t$  and  $Bi$ . Thus, for a fixed value of  $Y$ , the desired value of  $t$  is given by  $t = t^*/Bi$ ,  $Y$  being held constant. This essentially means that  $t$  varies inversely with  $Y$ . Hence, if the curves for  $Y$  versus  $t$  are plotted for all values  $Y$  and different  $Bi$ , they will be linearly shifted along the time scale a distance which is inversely proportional to the ratios of Biot numbers.

The modified successive approximation solutions (henceforth called exact) as plotted in Figures (4) and (5) do not exhibit the same behavior as the infinite thermal conductivity solutions. This deviation is because both the internal and surface resistance to heat transfer of the sphere are correctly represented in the exact solutions. Mathematically speaking, the temperature distribution in the exact case is given by equation (16), which can not be transformed to an equation independent of  $Bi$ . Hence the curves for the exact solutions are not shifted along  $t$  axis by the linear ratios of the Biot numbers.

Temperature-time curves for each Biot number along with the separable kernel approximations are shown graphically in Figures (6) through (13). The case for  $Bi = 0.1$  is also included in this set as a limiting case of small Biot number. A comparison of Figures (6) through (13) and Figure (4) reveals that the spread between the exact and the infinite thermal conductivity solutions increases with the increase of  $Bi$ .

$Bi$  can be interpreted as the ratio of the internal and external

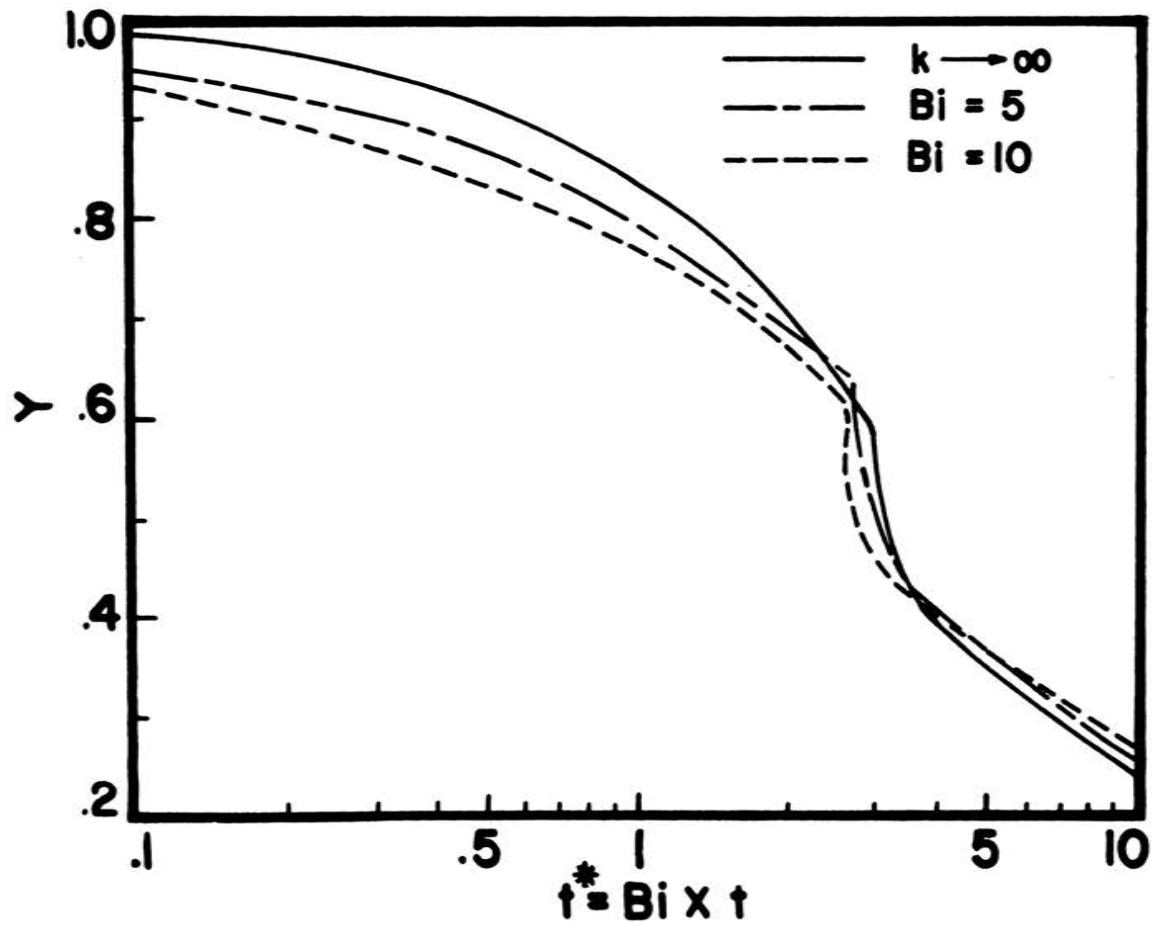


Fig. 5 Variation of Surface Temperature with the product of Biot Number and Time ( $Bi = 5$  and  $10$ ,  $k = \infty$  case).

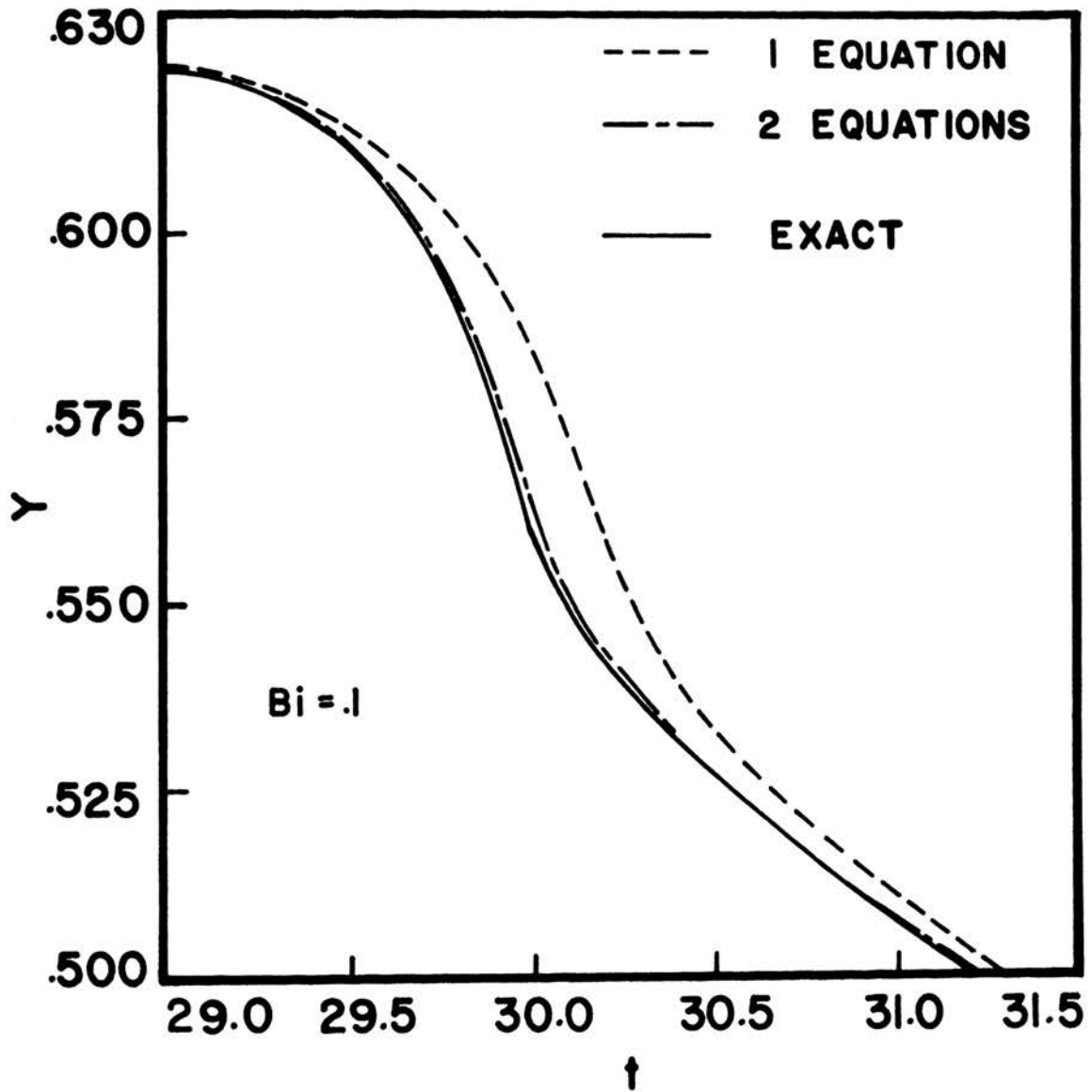


Fig. 6 Comparison between the Exact Solution and Separable Kernel Approximations ( $Bi = .1$ ).

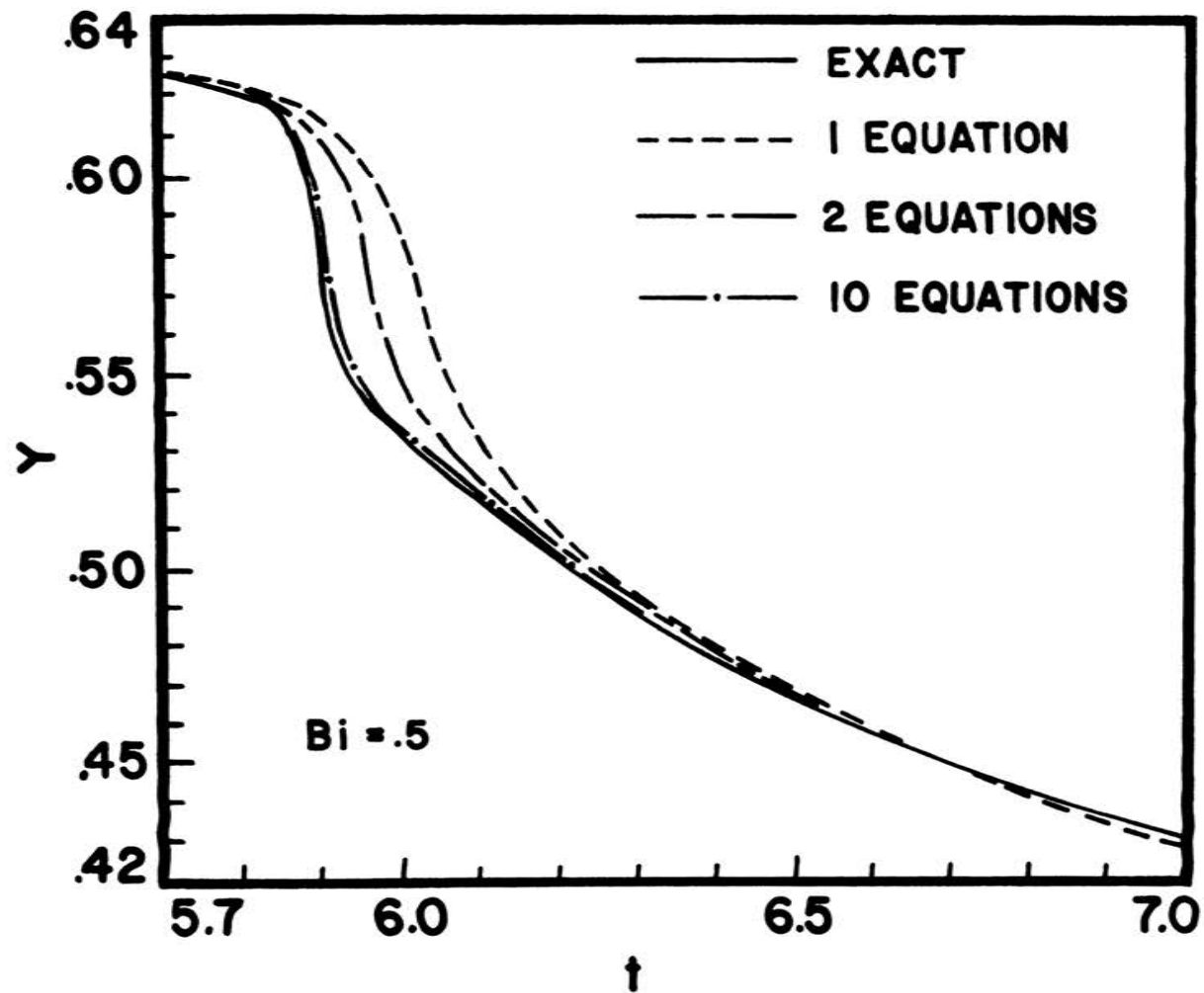


Fig. 7 Comparison between the Exact Solution and Separable Kernel Approximations ( $Bi = .5$ ).

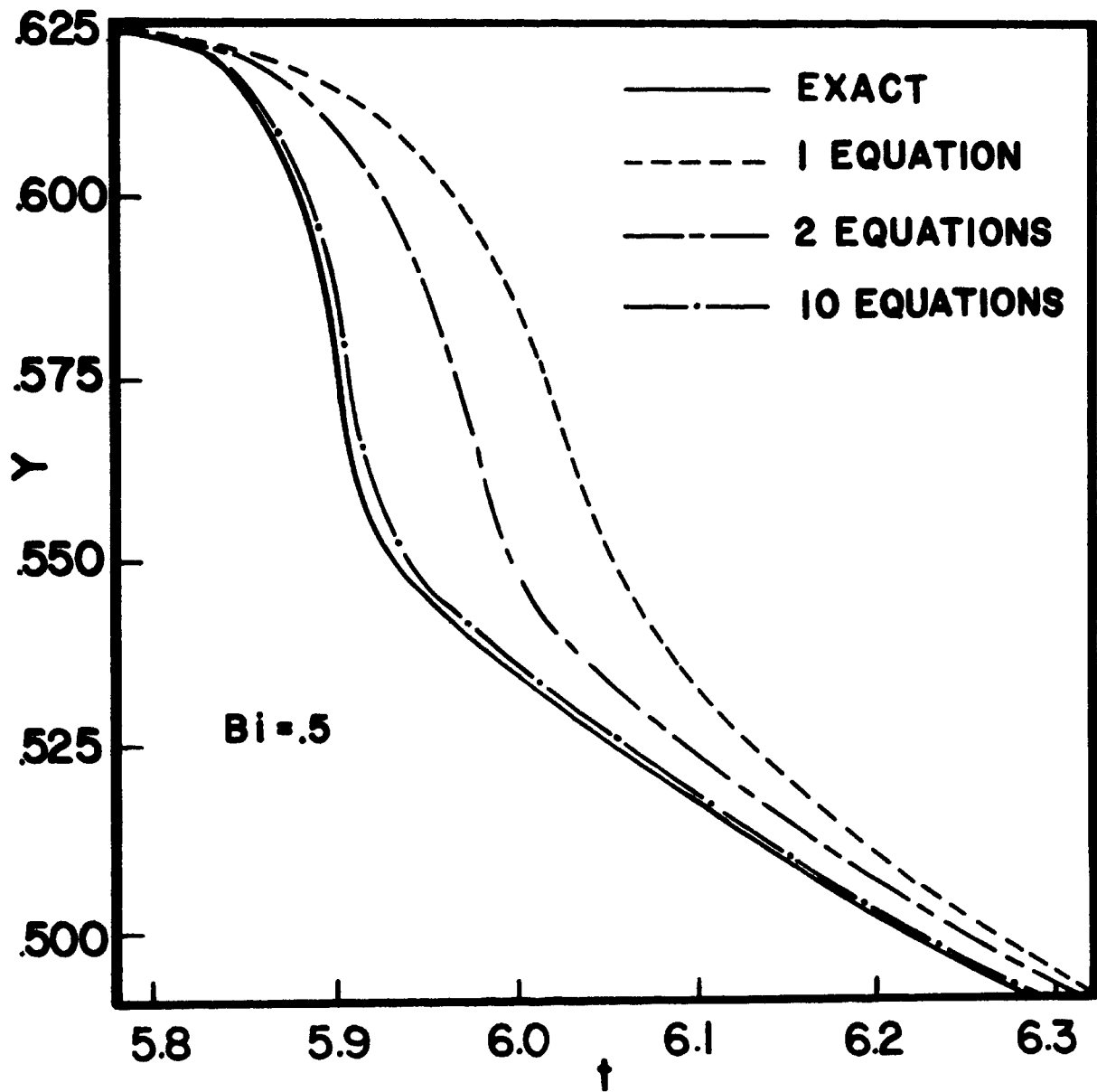


Fig. 8 Comparison between the Exact Solution and Separable Kernel Approximations ( $Bi = .5$ , large scale).



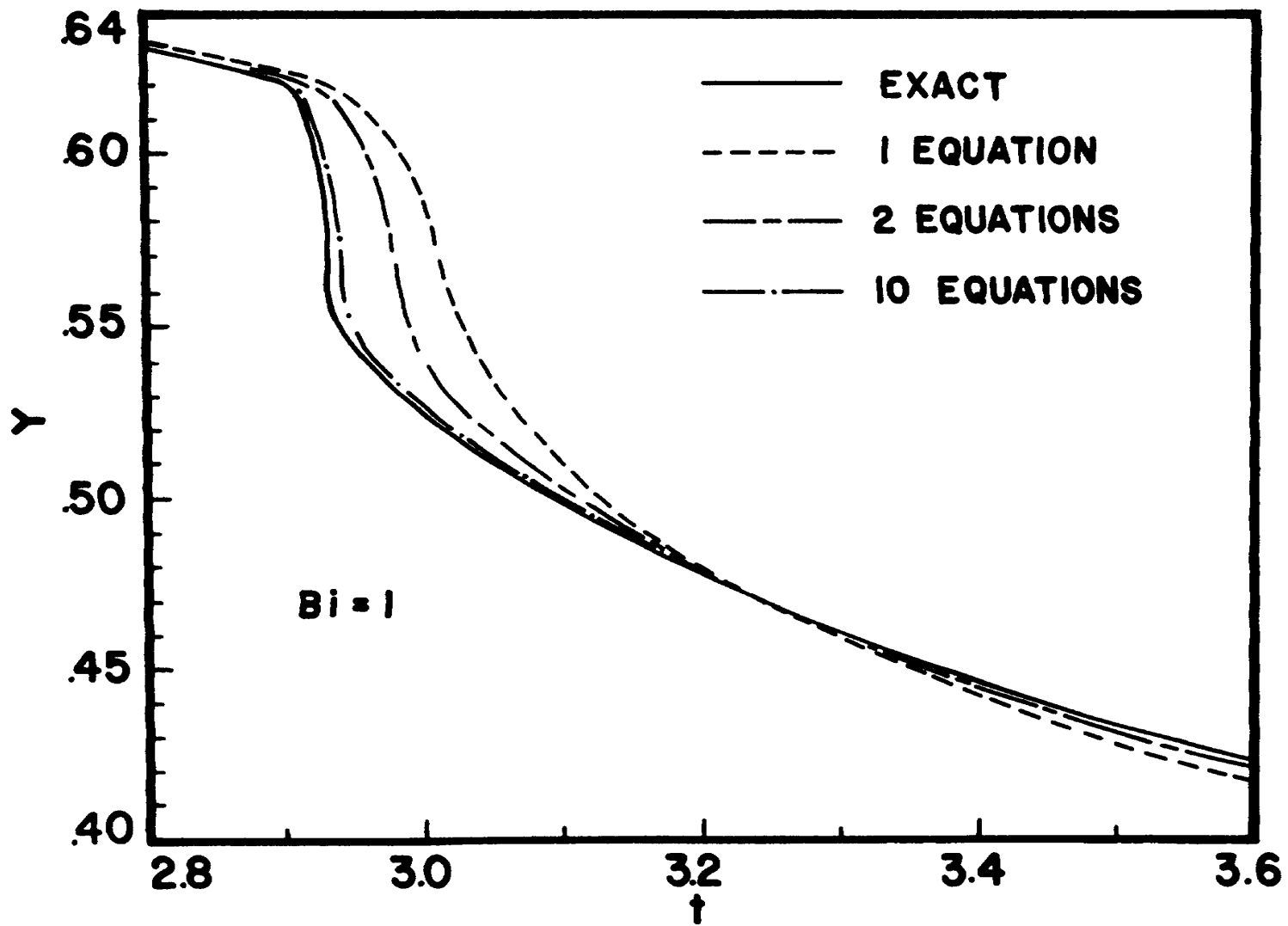


Fig. 9 Comparison between the Exact Solution and Separable Kernel Approximations ( $Bi = 1$ ).

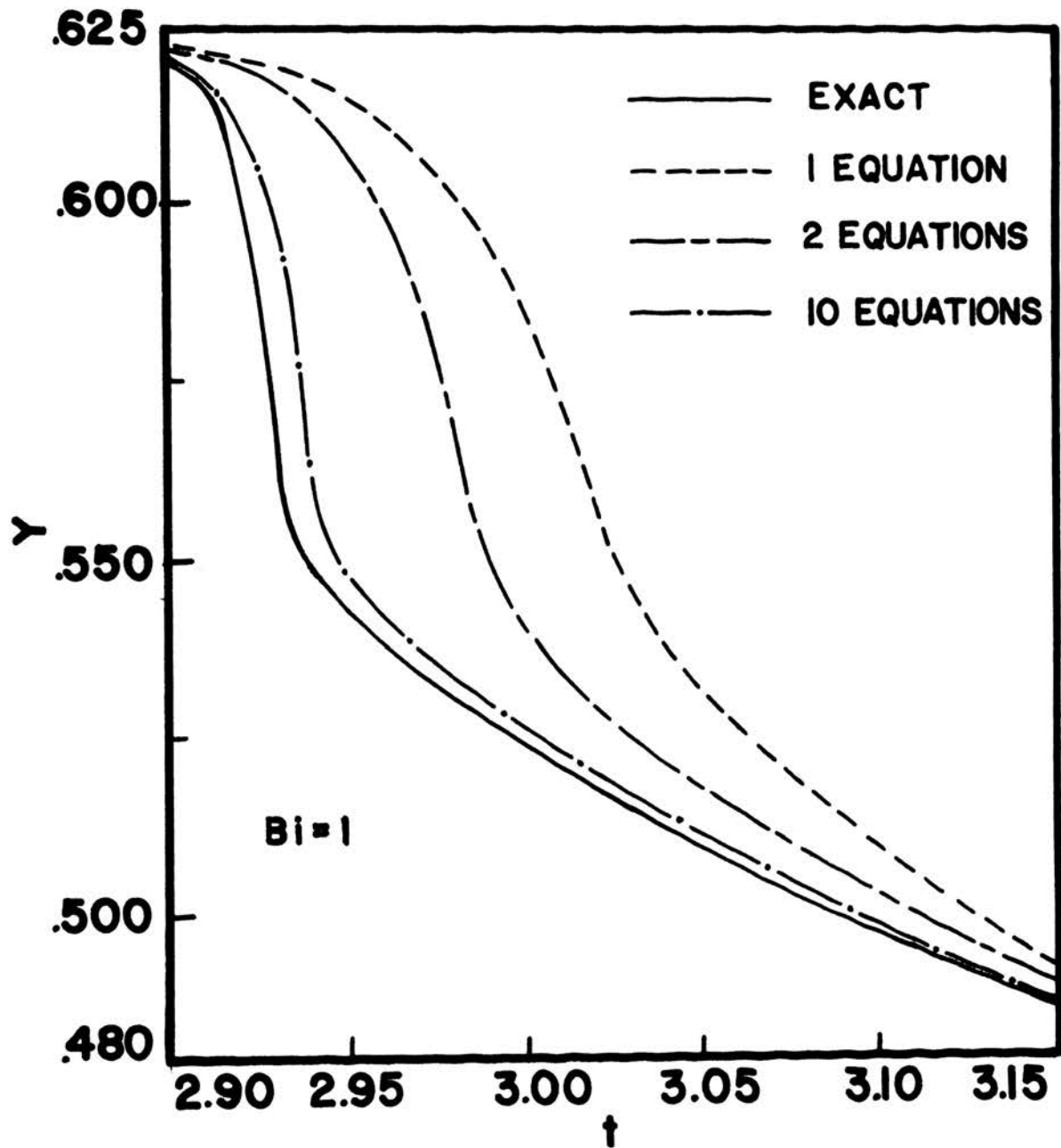


Fig. 10 Comparison between the Exact Solution and Separable Kernel Approximations ( $Bi = 1$ , large scale).

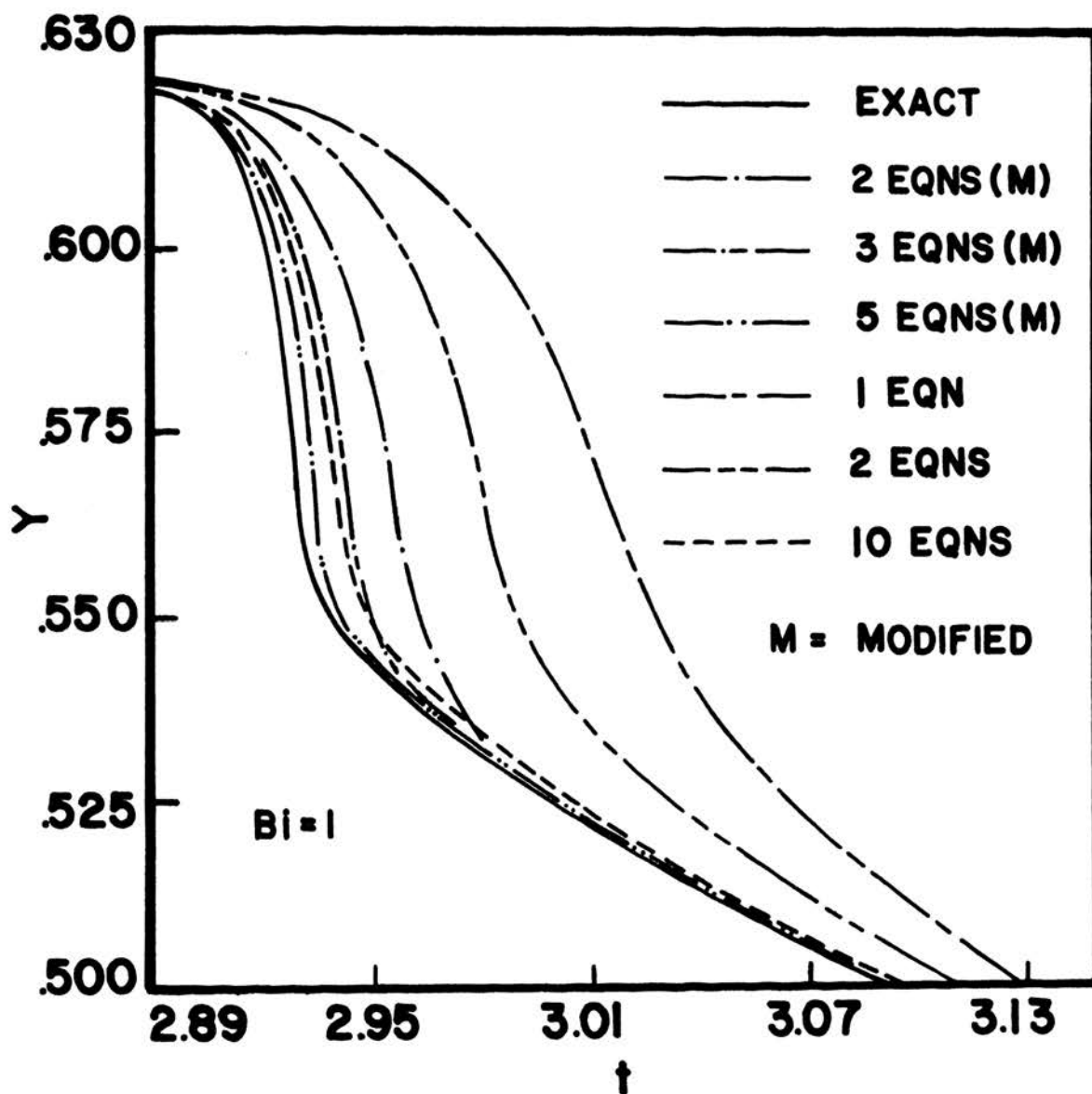


Fig. 11 Comparison between the Exact Solution and Separable Kernel Approximations ( $Bi = 1$ , large scale with some Modified Separable Kernel Method Solutions).

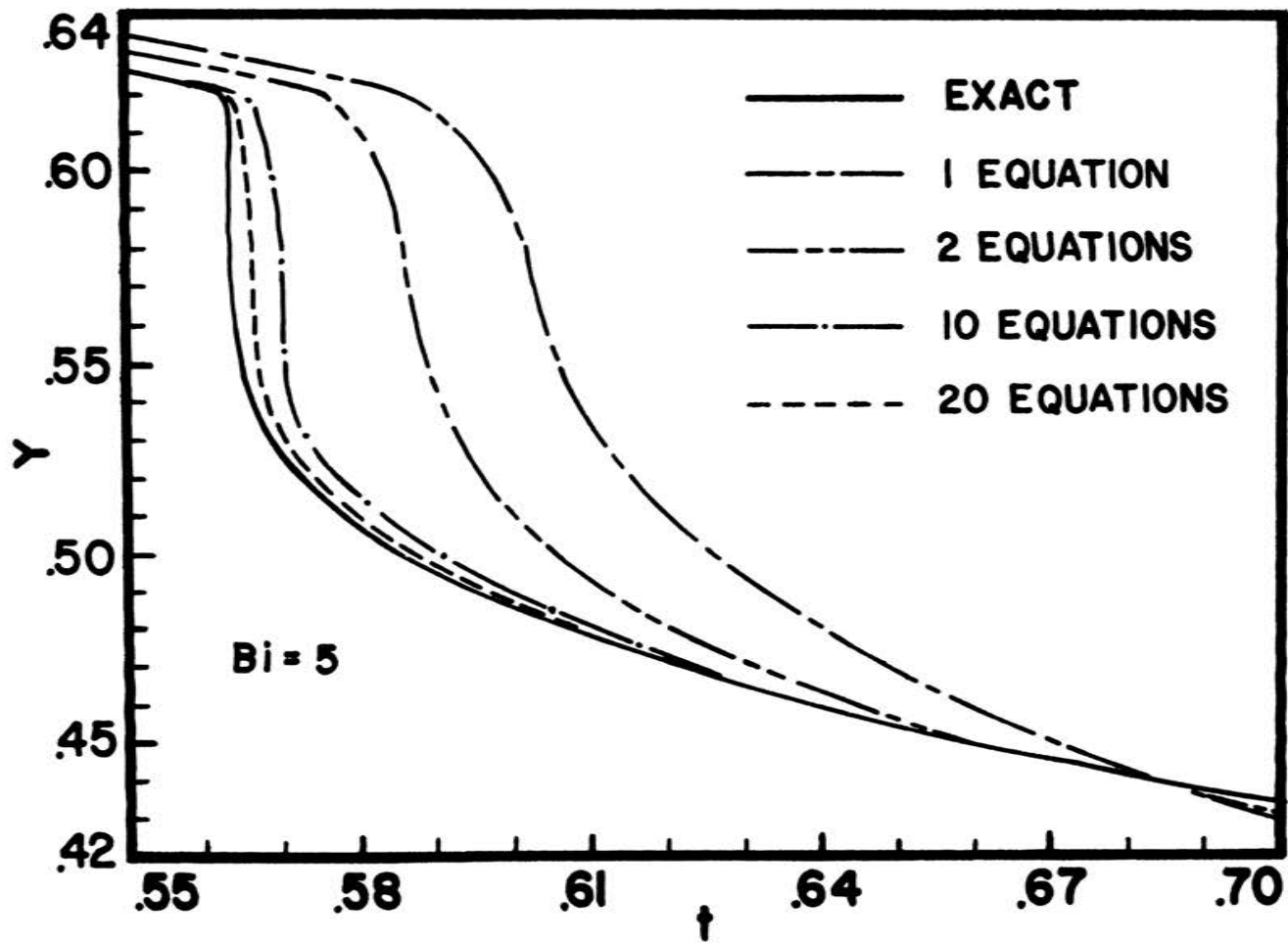


Fig. 12 Comparison between the Exact Solution and Separable Kernel Approximations ( $Bi = 5$ ).

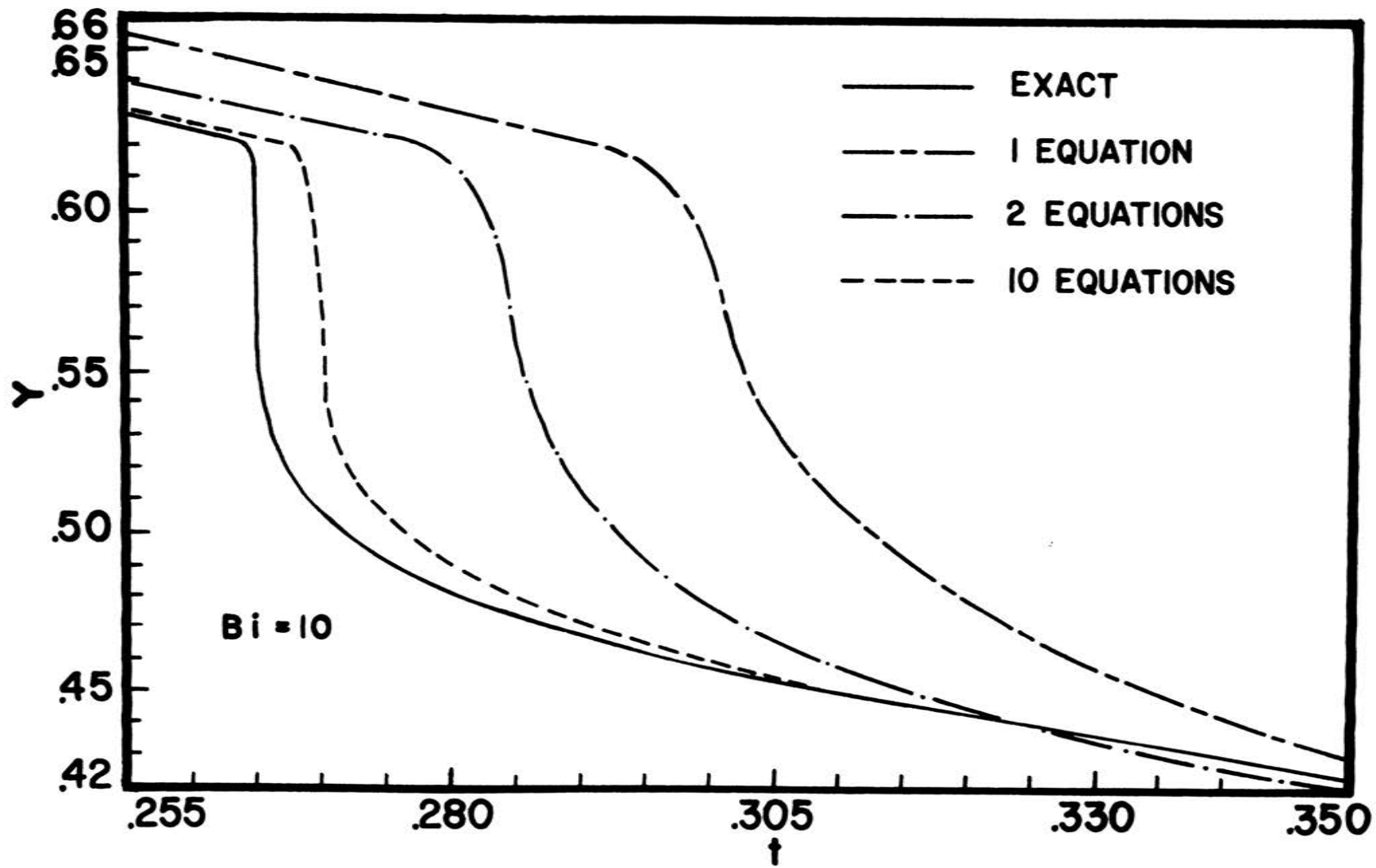


Fig. 13 Comparison between the Exact Solution and Separable Kernel Approximations ( $Bi = 10$ ).

resistance to heat transfer of the solid concerned. The infinite thermal conductivity solution is based on a zero internal resistance assumption. As the Bi increases, the internal resistance becomes progressively comparable with the external resistance. Hence with the increase of Bi, the exact solution increasingly shifts away from the ideal approximation of a zero internal resistance and thus the spread between the two solutions become apparent.

For  $Bi = 10$ , the spread, particularly in the region where a sudden drop in temperature takes place (henceforth will be called critical region in this study), is much larger than for  $Bi = 0.10$ . This essentially means that during cooling, the infinite thermal conductivity solutions compare poorly with the exact solution for large Biot numbers. But with a decrease of Bi, as seen in Figures (6), (7) and (9), the infinite thermal conductivity solutions tend to approach the exact solutions. Therefore, for the small Biot number case, as can be seen from Figure (6) for  $Bi = 0.10$ , the exact solution can be approximated by the infinite thermal conductivity assumption. Figures (6), (7) and (9) represent the temperature distribution on the surface of a sphere for a wide range of time for three different Biot numbers (0.10, 0.50 and 1.0) whereas the rest of the Figures in the set (6) through (13) indicate the temperature distribution for the critical region in a much larger scale for four different numbers ( $Bi = 0.5, 1.0, 5$  and  $10$ ).

It is to be observed that the spread between the exact and the infinite thermal conductivity solution is particularly noticeable in the critical regions (most of the nucleate and transition boiling regimes), where a large change in temperature occurs with a small

change in time. This can be explained from the  $h - T_g$  curve, Figure (3). In this curve, the heat transfer coefficient has a sharp peak around  $900^\circ$  F. Hence, in the vicinity of this temperature, a major portion of the energy is lost from the solid and consequently a sharp drop in temperature takes place. But the infinite thermal conductivity solution is based on the assumption of a uniform temperature throughout the solid. Hence, to maintain the uniformity of the interior temperature, the response of the solid to the sudden changes in the heat transfer coefficient at the surface, has to be slower than the exact solution. Therefore, in the case of the infinite thermal conductivity assumption, the critical region occurs at a later stage than in the exact solution. The drop in temperature also becomes smoother.

As can be seen in Figures (6) through (13), the infinite thermal conductivity solutions always indicate higher values of temperatures than the exact solutions for the same values of time up to a certain point. But at some point well beyond the critical region, the infinite thermal conductivity solution crosses the exact solution and indicates lower values of temperature than the exact solution along the time scale. Although solutions for large time have not been shown in these graphs, numerical results indicate that for large time, the infinite thermal conductivity solution very nearly coincides with the exact one.

The above-mentioned behavior of the infinite thermal conductivity solution can be explained in the following manner. At the end of the cooling, the sphere must have reached the bath temperature regardless of whether or not the infinite thermal conductivity

assumption has been included in the model. During the entire process of cooling, an equal amount of energy is lost for both the cases. The heat loss is proportional to the area below the corresponding Y versus t curves. Hence, if in the earlier part of cooling, the infinite thermal conductivity solution indicates higher values of temperature along the time scale, during the later part of cooling it must indicate a lower value of temperature than the exact solution. At some intermediate point, therefore, the infinite thermal conductivity solution must cross the exact solution.

It is seen from Figures (6) through (13), that as Bi is increased, the dip in the critical region becomes steeper and steeper. In the case for  $Bi = 10$ , there is a very sharp drop in temperature at  $t = 0.264$  with almost no change in dimensionless time. This sharp drop can be attributed by the fact that with the increase in Bi, the total time region ( $t = \alpha t_1/R^2$ ) for cooling has been shrunk and correspondingly, the time range for the critical region has also been reduced. But the same temperature drop must take place during the reduced dimensionless time range. Hence the Y - t curves become steeper with the increase of Bi.

Separable kernel solutions with more than one equation are also presented in graphical form in Figures (6), (8) and (10) through (13). As the number of equations is increased, the separable kernel solution seems to approach the exact solution. The reason for this behavior is simple. With an increase in the number of equations, the kernel is represented more accurately. However, an indefinite increase in the number of equations is undesirable because the rate



of convergence of the separable kernel method to the exact solution becomes progressively slower with an increase in the number of equations. This means that the change in the rate at which the separable kernel method approaches the exact solution resulting from the increase in the number of equations from 10 to 20 is much less than the change in the rate resulting from an increase in the number from 1 to 2. Hence, it is expected that a stage will be reached when virtually no improvement in the efficiency will be observed by increasing the number of equations. In the present study, solutions for the separable kernel method with up to 20 equations have been presented.

Values of surface temperature are also computed by the modified separable kernel method for  $Bi = 1$ . For comparison purposes, these are presented in Figure (11) along with the ordinary separable kernel method and the exact solutions. The increase in efficiency with the use of the modified method over the ordinary one is obvious from this figure. The modified method needs only 3 equations to attain almost the same solution as the ordinary method with 10 equations. Also, the modified method gives a much closer approximation to the exact solution with just 5 equations than the ordinary method with 10 equations. The same kind of behavior can be expected for other Biot numbers.

Surface heat fluxes for different Biot numbers have been determined numerically and plotted against time in Figures (14) and (15). Full logarithmic graphs have been used for the plots because of the large variation in the heat flux with temperature. A brief descrip-

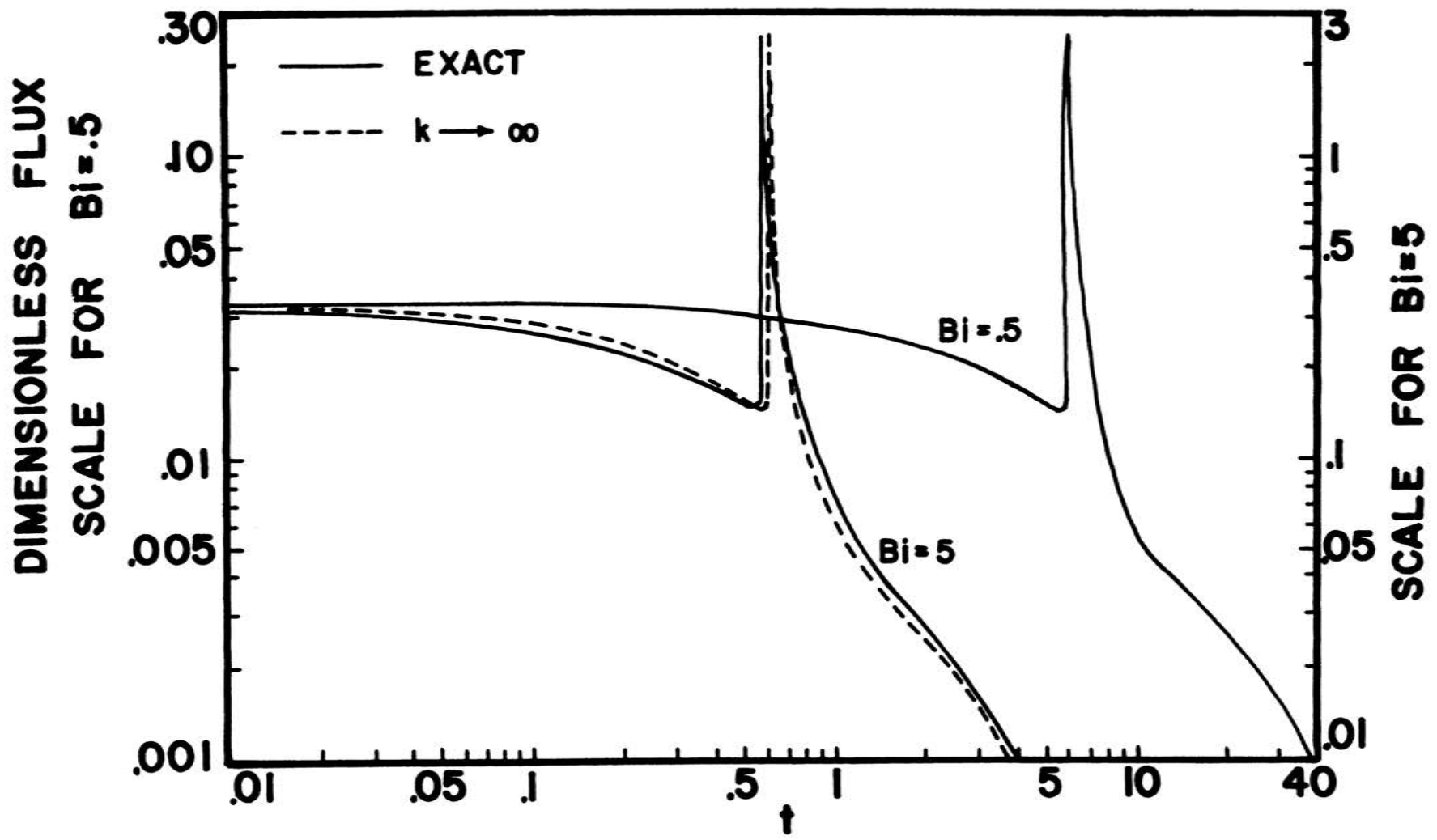


Fig. 14 Variation of Heat Flux with Surface Temperature ( $Bi = .5$  and  $5$ ).

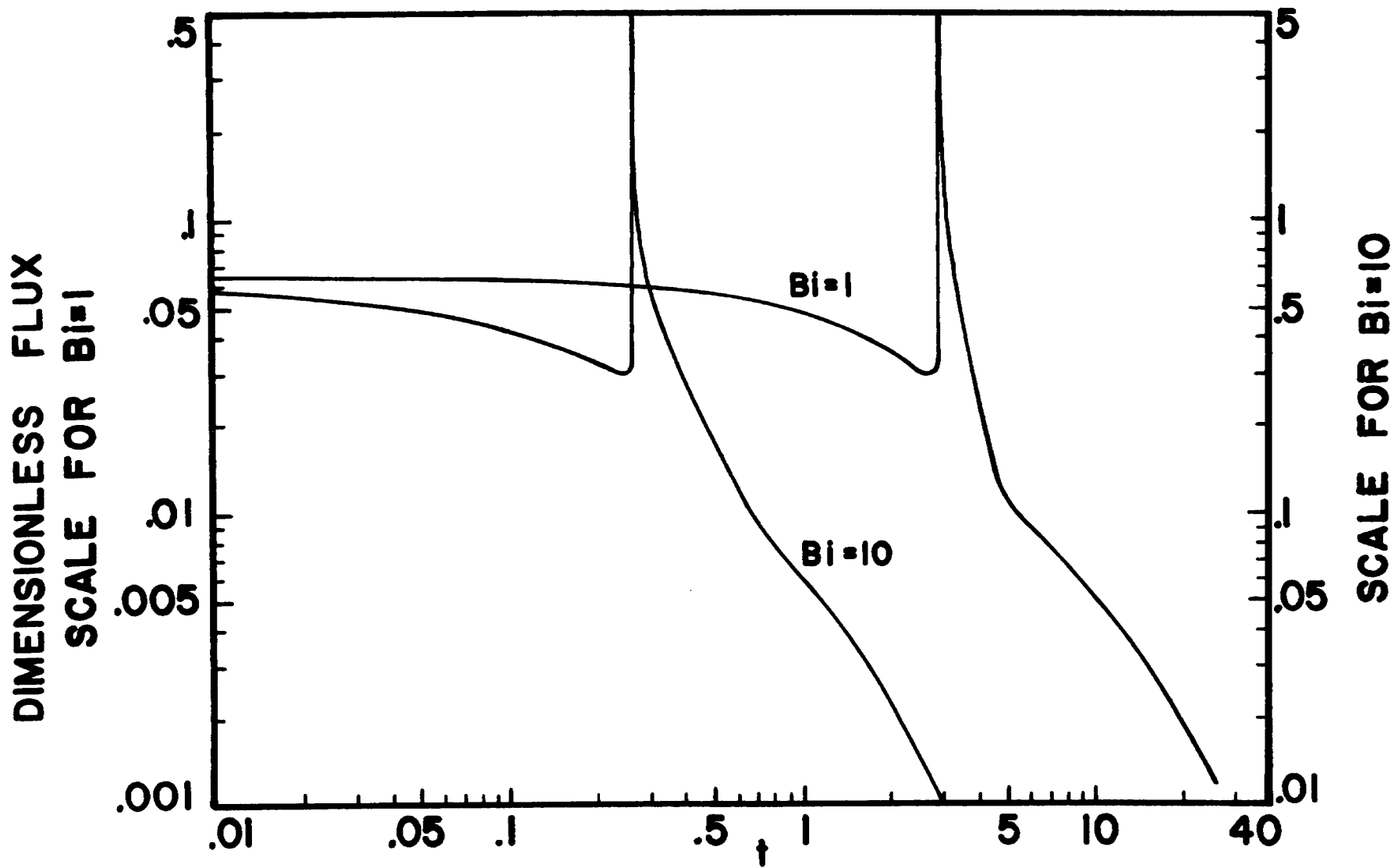


Fig. 15 Variation of Heat Flux with Surface Temperature ( $Bi = 1$  and  $10$ ).

tion of the numerical method for the determination of the heat fluxes seems necessary here. The determination of heat transfer coefficient  $h$  has already been discussed. Once the surface temperature  $Y$  for a particular time is known, the value of  $h$  corresponding to that surface temperature can be determined from Figure (3) or by numerical interpolation if a better accuracy is desired. The product of  $h$  and the temperature difference between the sphere and the liquid, therefore, determines the flux at a particular time.

In Figure (14), heat fluxes for the infinite thermal conductivity solution in the case of  $Bi = 5$  have also been calculated and compared with the exact solution. As expected from the temperature behavior from the preceding Figures (5) through (13), there is a sharp peak in each of these four graphs of heat flux versus time representing a small region where the heat flux is well above the average value (peak nucleate boiling regime). This peak indicates a large loss of energy during a small period of time. These spikes become steeper and steeper with increasing  $Bi$  which again is consistent with the temperature behavior. It is also noted that, for large time, the heat fluxes become negligibly small compared to the average value of the flux. This is explained by the fact that at large time, the temperature difference between the solid and the coolant becomes very small and the value of  $h$  is also considerably reduced with the reduced surface temperature of the solid, Figure (3). The heat flux for the infinite thermal conductivity solution for  $Bi = 5$ , as shown in Figure (14), closely follows the exact solution. But the position of the peak heat flux is shifted towards the right along the time scale and at some point beyond this peak heat flux position,

the value of the heat flux for the infinite thermal conductivity solution continues to be less than the exact solution. This behavior is again consistent with the temperature behavior of the infinite thermal conductivity solution discussed previously.

The time rate of change of the surface temperature indicates how rapidly the surface of the sphere cools. These rates ( $dY/dt \doteq \Delta Y / \Delta t$ ) have been calculated from the numerical results of the surface temperatures by forward and central difference techniques. The calculation of  $dY/dt$  is important because it is frequently used for the determination of  $h$  from experiments. In experiments, normally the temperatures are measured and hence  $Y$  and  $dY/dt$  can be evaluated. With the assumption of a thermally lumped solid, heat flux is then determined. In mathematical form this can be expressed as

$$q/A = -(M c_p / A) dT/dt_1$$

where  $q/A$  is the heat transfer per unit area  
and  $M$  is the mass of the solid.

Division of the heat flux by the temperature difference between the surface of the solid and the liquid then yields the heat transfer coefficient  $h$ . Small or hollow spheres are commonly used in the experiments so that the assumption of a thermally lumped solid (i.e. infinite thermal conductivity assumption) can be made.

The rates have been calculated for both the exact and infinite thermal conductivity solutions for the Biot numbers of 0.1, 0.5, 1.0, 5 and 10 and are plotted in Figures (16) through (20). It is observed from these graphs that only in case of small Biot numbers

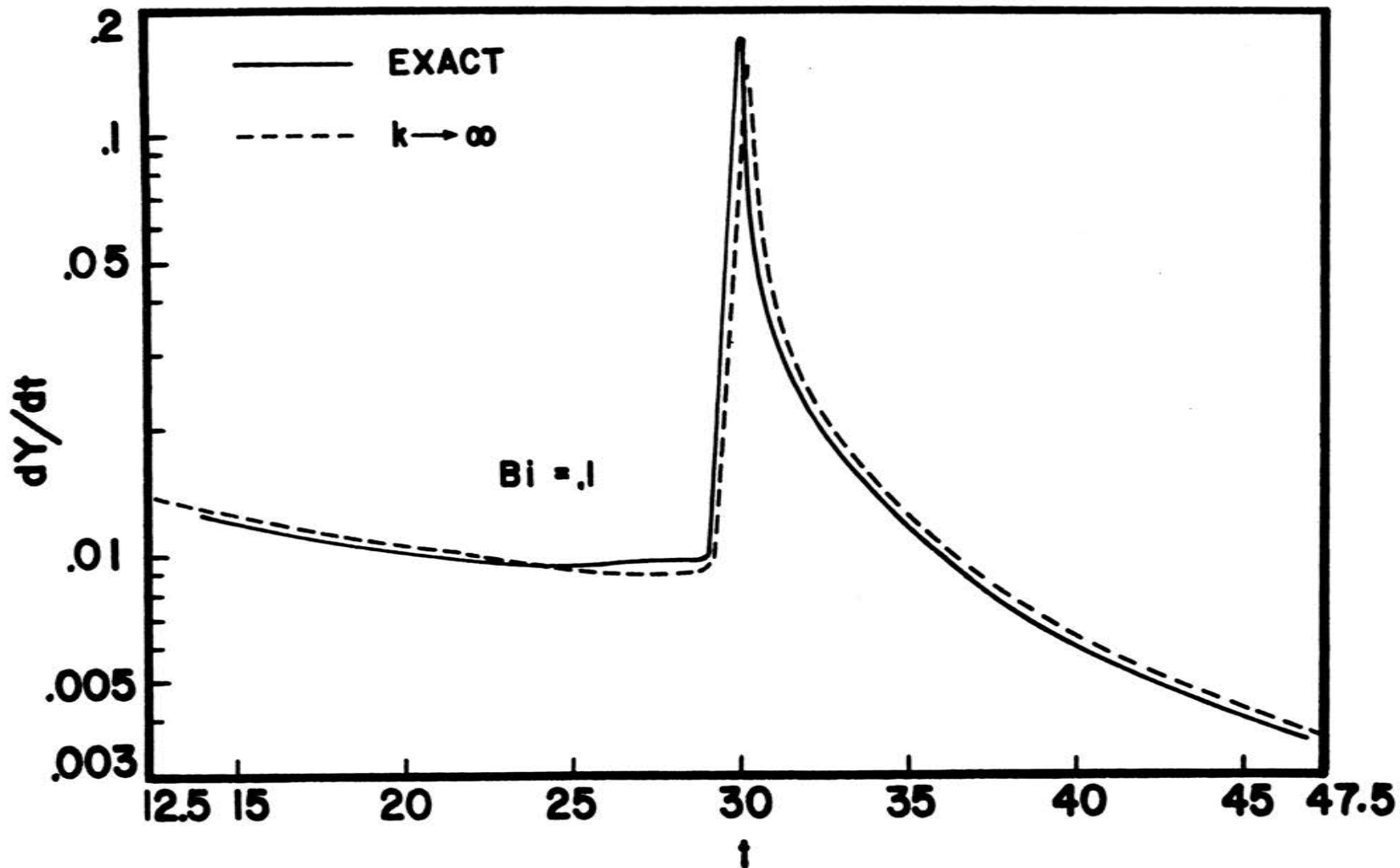


Fig. 16 Time Rate of Change of the Surface Temperature with Time for both the Exact and Infinite Thermal Conductivity Case ( $Bi = .1$ ).

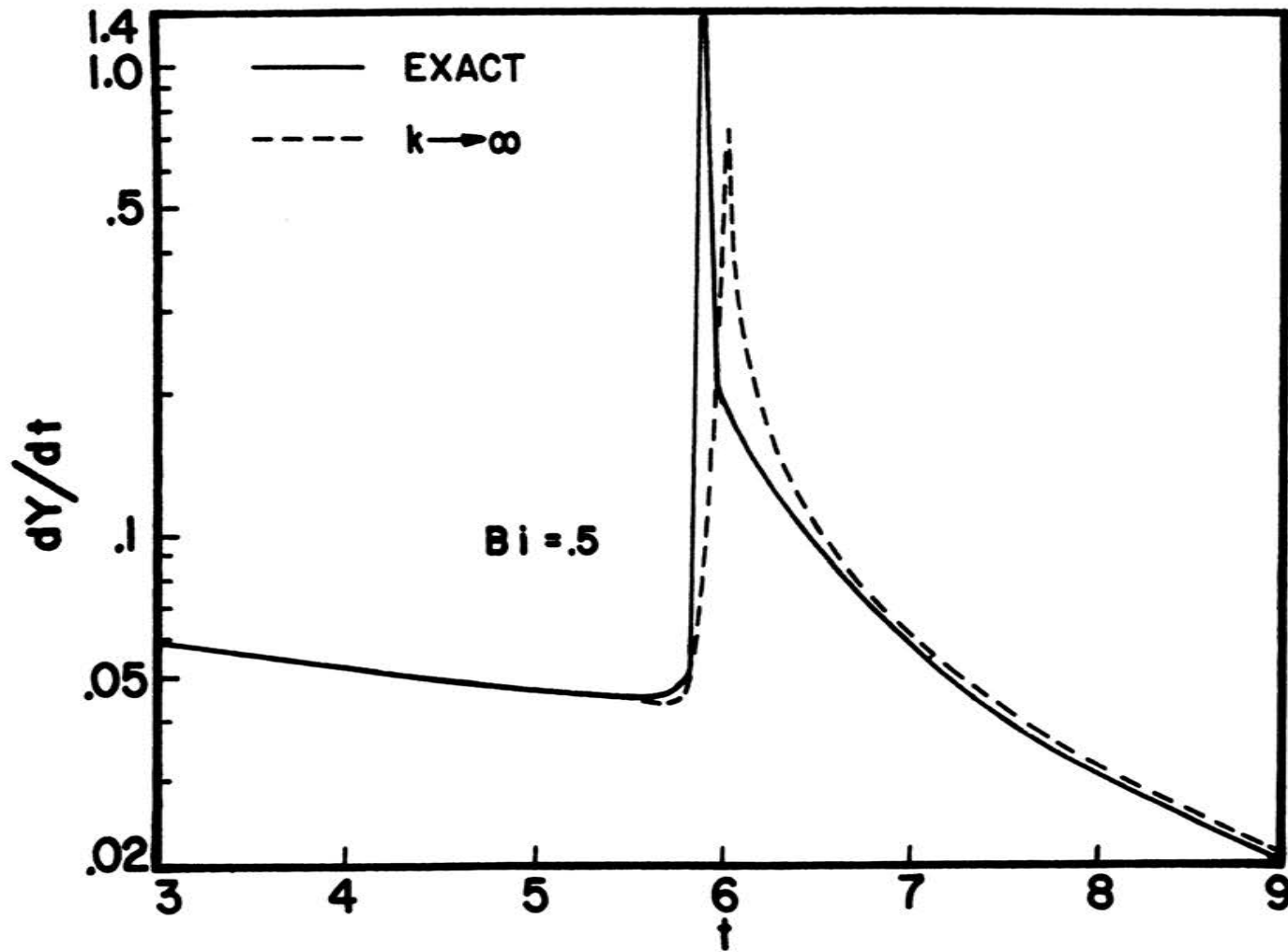


Fig. 17 Variation of the Time Rate of Change of the Surface Temperature with Time for both the Exact and Infinite Thermal Conductivity Case ( $Bi = .5$ ).

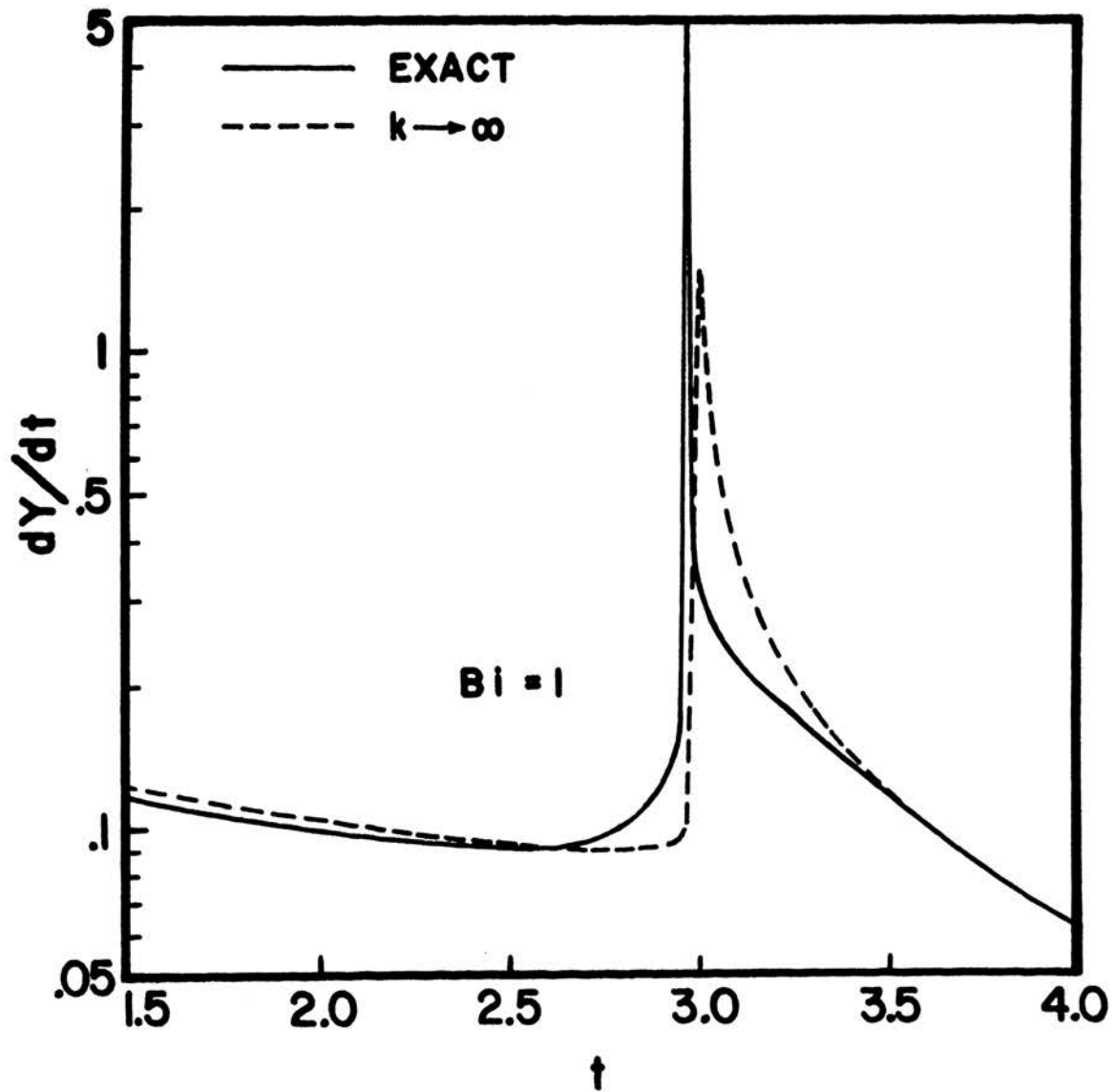


Fig. 18 Variation of the Time Rate of Change of the Surface Temperature with Time for both the Exact and Infinite Thermal Conductivity Case ( $Bi = 1$ ).



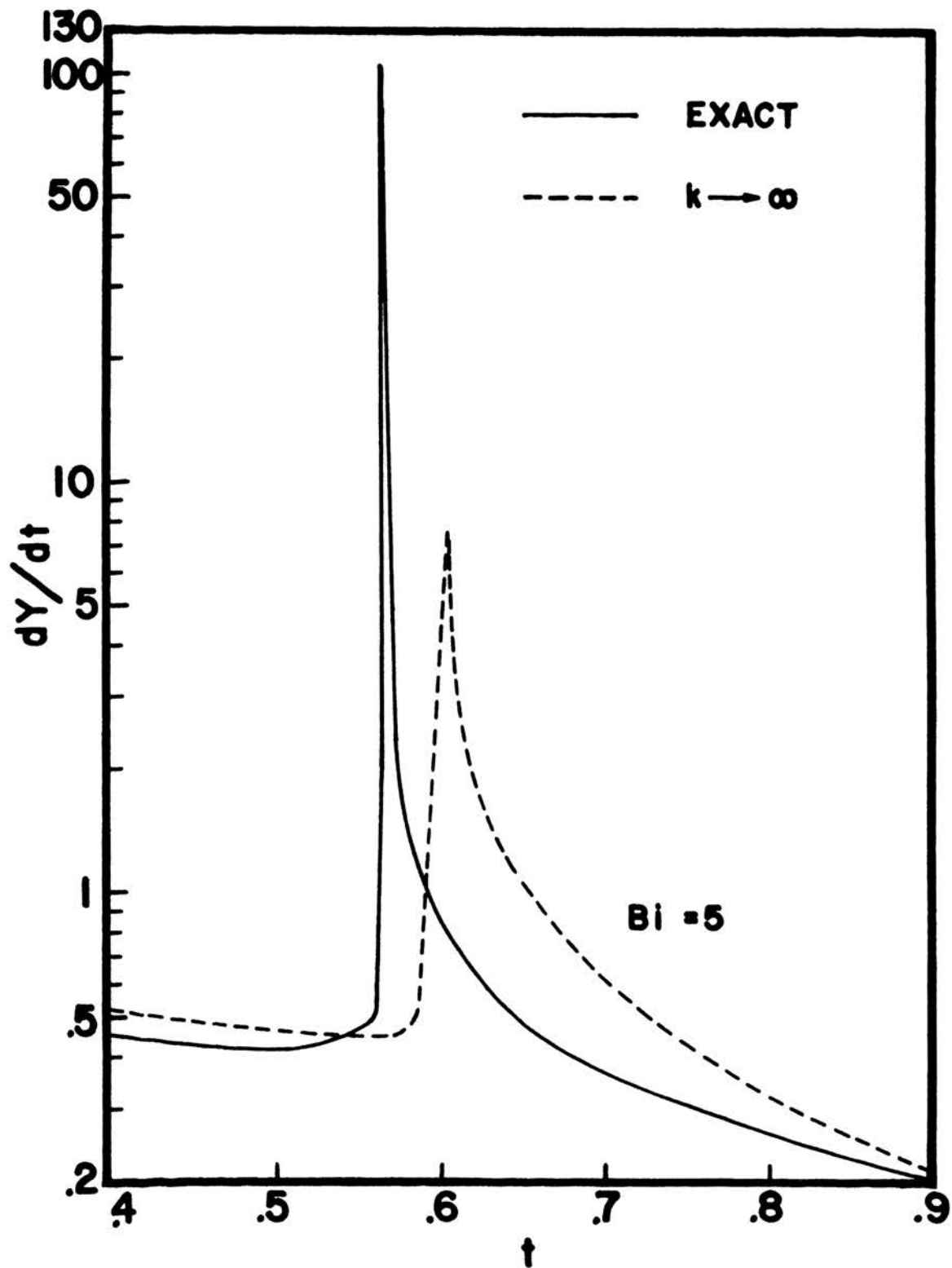


Fig. 19 Variation of the Time Rate of Change of the Surface Temperature with Time for both the Exact and Infinite Thermal Conductivity Case ( $Bi = 5$ ).

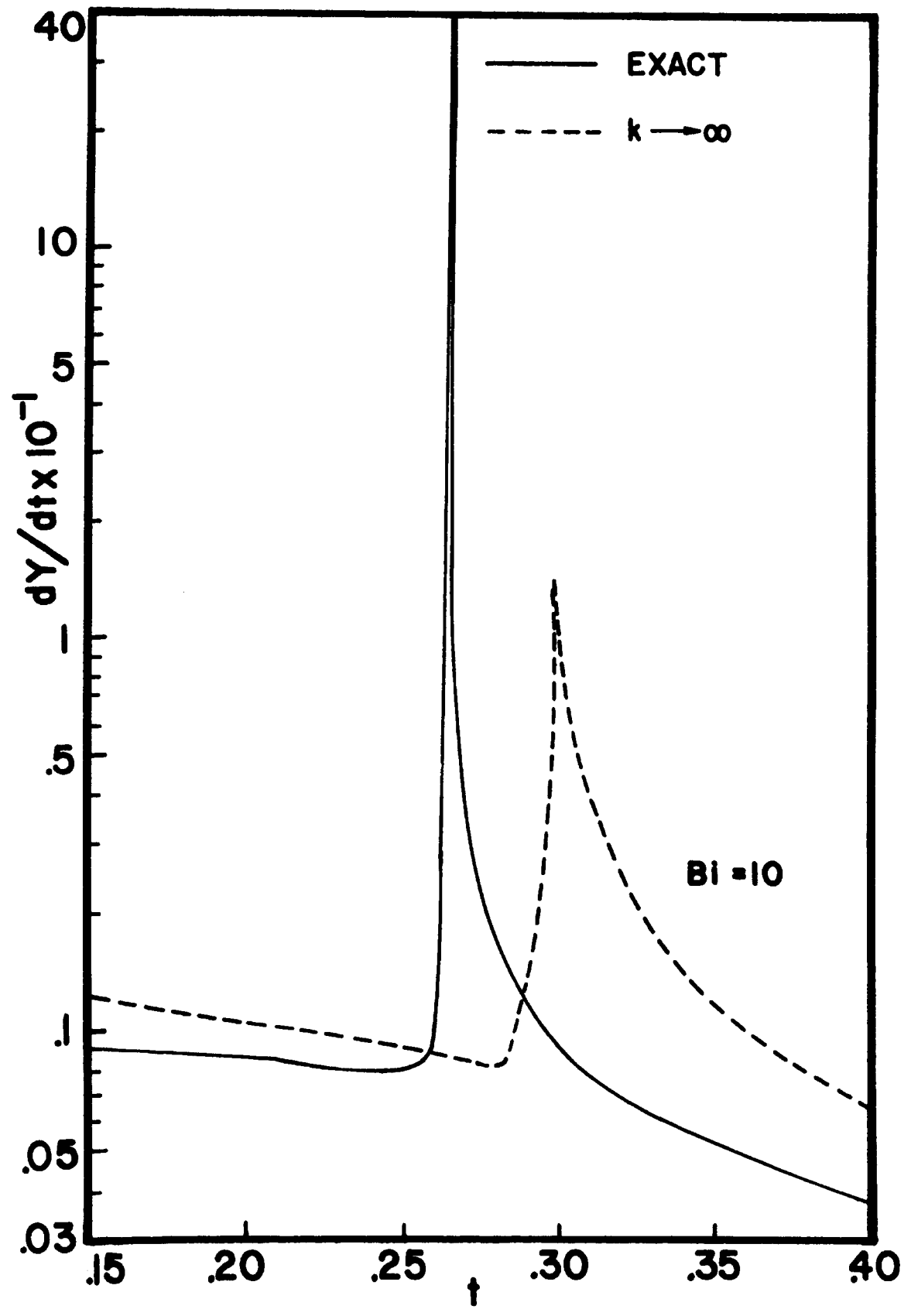


Fig. 20 Variation of the Time Rate of Change of the Surface Temperature with Time for both the Exact and Infinite Thermal Conductivity Case ( $Bi = 10$ ).

(0.1 and 0.5), the exact and infinite thermal conductivity solutions are very close to each other. The exact solution can be approximated by the infinite thermal conductivity solution for these cases. With the increase of Bi, however, the infinite thermal conductivity assumption breaks down in comparison with the exact case, particularly in the regions of the sharp rise of the magnitude of the derivatives or in the peak regions. In these regions, the error between the infinite thermal conductivity solution and the exact solution is more than 400% for Biot numbers of 5 and 10 and the location of the peak for the infinite thermal conductivity solution occurs much later than the exact solution. Although this error for  $Bi = 1.0$  is of the order of 300% in the peak regions, for the remaining portion of the curve, the infinite thermal conductivity solution closely follows the exact solution. Hence, for the  $Bi = 1.0$  case, the infinite thermal conductivity solution can be used with a less than 10% deviation from the exact solution except in the region around the peak value of the curve.

It is to be noted that the curves of Figures (16) through (20) are similar in shape to the heat flux versus time curves, Figures (14) and (15). But the peaks of these derivatives seem to have sharper rise than the heat flux cases. As expected, the peaks of the infinite thermal conductivity solutions are shifted to the right from the exact solution along the time scale. With the increase in Bi, the shift between the exact and the infinite thermal conductivity solutions become more and more pronounced. This shift is due to the very nature of a zero internal resistance assumption in the solid. The solid under this assumption is always in a process

of maintaining a uniform temperature throughout. Hence, in maintaining this criterion, more time will be needed for the solid to adjust itself to the sudden changes in the surface conditions than the exact solution. Hence, if the Biot number is increased (i.e. by increasing the diameter of a solid), the solid will take more time to adjust itself for maintaining a uniform condition to the sudden change in the surface condition. Thus, the peak will be more and more shifted to the right with the increase of  $Bi$ .

It has been mentioned that both the forward and central difference techniques have been employed for the calculation of  $dY/dt$ . Some improvement in the results was observed, particularly in those regions where a change in time step was made, by the application of central difference over the forward difference technique. This is quite understandable since the central difference computation is based on the information from both sides of the point at which the value is to be computed whereas the information from only one side of the point is required for the forward difference computation.

A few words of caution should be mentioned about computer time. It has been found that to attain a reasonable amount of accuracy in case of a large  $Bi$  (say 10), a considerable amount of computer time is required for the successive approximation method. Cases for Biot numbers greater than 10 were not calculated in this study. However, from the trend of the computer time spent on  $Bi = 0.1, 0.5, 1, 5$  and 10, it can be inferred that for very large Biot numbers (say 50 or 100), a large amount of computer time would be required. Computer time does not vary directly with the ratios of Biot numbers but progressively increases with the increase of  $Bi$ . However, this is

not a unique disadvantage of the successive approximation method, since this will essentially be true for all other numerical methods because of the sensitive nature of the Y versus t curve. Also for large Biot numbers, a careful choice of time steps has to be made, particularly in the critical region. Otherwise the solution will fail to converge within a finite number of iterations. This choice of step size does not follow the linear ratios of Bi. Suitable time steps have to be determined by trial and error and experience. This is a painstaking and laborious process and requires a lot of computer time. Again this is not a limitation for this particular method since this is true for all other numerical techniques.

## VI CONCLUSION

A practical method for obtaining an 'exact' solution for the unsteady state temperature distribution in a sphere subject to a nonlinear convective boundary condition has been presented. Surface temperature results for different Biot numbers are presented in graphical form and compared. Heat flux and rate of change of temperature with respect to dimensionless time (Fourier number) are also calculated for different Biot numbers and a comparative study has been made. Two approximate methods of solution for the surface temperature have been proposed and the modified separable kernel method has been found to be more efficient than the ordinary one. The limiting case of infinite thermal conductivity solution is also investigated and found to give good results for large time.

The modified successive approximation method as presented in this thesis, can take into account any change in geometry of the solid and a wide range of temperature between the solid and the coolant. However, as a prerequisite to the problem, values of heat transfer coefficient  $h$  must be known for all temperatures in order to fulfill the requirement of a complete set of boundary conditions, equations 4(a), (b), (c) and (d). With known values of  $h$ , the techniques presented in this study, can be used to calculate the surface and thereby the interior temperature, for different Biot numbers.

The accuracy of the numerical techniques used for the solution of equation (16) is good enough for all practical purposes. Where a high degree of accuracy (within 1 to 2 percent of the exact solution)

is not desired, either of the separable kernel methods can be used to the best advantage. A large number of equations essentially increases the efficiency of either of the separable kernel methods but this also necessitates the determination of an equal number of eigenvalues and the solution of a large number of interlinked differential equations. Hence a suitable compromise should be made.

From the discussion of the results, it can be conveniently concluded that for the cases of Biot numbers higher than one, the infinite thermal conductivity solution breaks down compared with the exact one. The error in approximation becomes significantly large in the critical region (or the nucleate boiling region) where a rapid rate of heat flow is observed. However, the error is considerably less for Biot numbers less than 1.0. Hence, for the case of Biot number less than one, the exact solution can be approximated by the simple assumption of lumped thermal system.

In the previous chapter, it has been discussed how the time rate of the change of the surface temperature ( $dY/dt$ ) is calculated and a comparative study of these rates for different Biot numbers has been presented. The knowledge of  $dY/dt$  is useful, particularly for the smaller Biot number cases. For a small Biot number, the sphere can be assumed to be thermally lumped and hence the simple form of the heat flux expression  $q/A = (-Mc_p/A) dT/dt_1$  can be applied. With the knowledge of the heat flux, the heat transfer coefficient  $h$  can be easily determined. Normally in experiments, small spheres are used to ensure a small Biot number so that the approximation of a thermally lumped solid can be made. This avoids a lot of lengthy and laborious calculation.

As mentioned previously, this particular method of solution is flexible enough to account for other one dimensional geometries. Hence a direct extension of the present problem can be the solution for the temperature history of a slab, cylinder or a semi-infinite solid subjected to nonlinear convective boundary conditions. This can be accomplished simply by changing the expressions of the kernels for different geometries, equations (24), (25) and (26) and substituting in equation (16) for the determination of the surface temperature corresponding to that particular geometry. Eigenvalues for the different geometries will also be different. In the present problem, the interior temperature history of the solid has not been sought, although the method for its determination has been briefly discussed in the previous chapter. Thus, the avenue for the exploration of the interior temperature of the sphere and other geometries is left open. With the knowledge of the interior temperature, a suitable comparison between the interior and the surface temperature of the solid for the particular cases can be made. In the process the response behavior of the solid to the changes in surface conditions can be obtained.

The present solution is based on the available heat transfer coefficient data for a paraffinic-type oil, designated as intermediate oil [1]. The same problem can be solved for different fluids, if heat transfer coefficient data is available for the entire range of boiling. Mention of the cryogenic fluids should be made here since heat transfer coefficient data for some of them are available. However, when cryogenic fluids are used as quenchents, proper steps must be taken to account for the temperature dependency of the



physical properties of the solid. The solution obtained by using a different fluid may be considerably different from the present solution depending upon the nature of the heat transfer coefficient - temperature curve, for the particular fluid.

VII BIBLIOGRAPHY

1. Stolz, G. Jr., Paschkis, V., Bonilla, C. F. and Acevedo, G., "Thermal Consideration in Oil Quenching", JISI 193, 116-123 (1959).
2. French, H. J., The Quenching of Steels, American Society for Steel Treating, Cleveland, Ohio (1930).
3. Paschkis, V. and Stolz, G. Jr., "Quenching as a Heat Transfer Problem", J. Metals 8, 1074-1075 (1956).
4. Stolz, G. Jr., "Numerical Solutions to an Inverse Problem of Heat Conduction for Simple Shapes", J. Heat Transfer 82, 20-25 (1960).
5. Heindlhofer, K., "Quenching, a Mathematical Study of various Hypothesis on Rapid Cooling", The Physical Review XX, 221-242 (1922).
6. Grossman, M. A., Ashimow, M. and Urban, S. F., in Hardenability of Alloy Steels, pp. 124-190, Cleveland, Ohio, ASM (1939).
7. Engel, N., Ingeniorvidenska Belige Skrifter, Serial No. A. 31, Copenhagen (1931).
8. Wever, F. and Rose, A., Mitt. Kaiser Wilhelm Institute 19, 289-298 (1937).
9. Rose, A., ibid 21, 181-196 (1939).
10. Russel, T. F., "Some Tests on Quenching Oils", ISI Spec. Rep. 24, 283 (1939).
11. Yoshida, T., Trans. Soc. Mech. Eng. (Japan) 16, 32-39 (1950).
12. Nakagawa, Y. and Yoshida, T., Trans. Soc. Chem. Eng. (Japan) 16, 74-82, 104-110 (1952).
13. Nakagawa, Y., Yoshida, T. and Kamitani, K., ibid 16, 405-412, 413-418 (1952).
14. Merte, H. and Clarke, J. A., "Boiling Heat Transfer Data for Liquid Nitrogen at Standard and Near-zero Gravity", Advances in Cryogenic Engineering 7, 546-550 (1962).
15. Veers, D. R. and Florschuetz, L. W., "A Comparison of Transient and Steady State Pool Boiling Data using the same Heating Surface", J. Heat Transfer 93, 229-232 (1971).

16. Paschkis, V., "The Coefficient of Heat Transfer during Quenching" (in German), Hart. Tech. Mitt. 15, 189-201 (1960), (Translation held by Aston University Library).
17. Carry, P. E., "A New Quenchant for Steel", Metal Progress 73, 79-81 (1958).
18. Harvey, R. F., "Ultrasonic Quenching", Ultrasonics 3, 149-151 (1965).
19. Taitz, N. U. and Kadinova, A. S., "The Hardening of Tubes by Water Jets", Stal in English, 525-527 (1960).
20. Budin, D. V. and Kondratov, V. M., "Quenching in Air-Water Mixtures", Metal Science and Heat Treatment, 367-370 (1965).
21. Paschkis, V. and Stolz, G. Jr., "How Measurements lead to Effective Quenching", The Iron Age 178, 95-97, Nov. 22 (1956).
22. Urusova, N. A. and Kurilekh, I. N., "An Investigation of the process of Heat Transfer with nozzle cooling in the Continuous Casting of Steel", British Iron and Steel Institute Translation No. 5165 (1965).
23. Sinnott, M. J. and Shyne J. C., "An Investigation of the Quenching characteristics of a Salt Bath", Trans. ASM 44, 758-774 (1952).
24. Bergles, A. E. and Thompson, W. G. Jr., "The Relationship of Quench Data to Steady State Pool Boiling Data", Int. J. Heat Mass Transfer 13, 55-58 (1970).
25. Jones, F. W. and Pumphrey, W. I., "Some Experiments on Quenching Media", JISI 156, 37-54 (1947).
26. Gaumer, G. R., "Stability of Three Finite Difference Methods of solving for Transient Temperatures", ARS Journal 32, 1595-1597 (1962).
27. Ivanov, V. V. and Salomatov, V. V., "On the Calculation of the Temperature Field in Solids with variable Heat Transfer Coefficients", J. Eng. Physics 2, 63-64 (1965).
28. Crosbie, A. L. and Viskanta, R., "Transient Heating or Cooling of One Dimensional Solids by Thermal Radiation", Proc. Third Int. Heat Transfer Conference 5, 146-153 (1966).
29. Crosbie, A. L., "Transient Heating or Cooling of One Dimensional Solids by Nonlinear Boundary Conditions", M.S. Thesis, Purdue University (1966).

30. Winter, D. F., "Transient Radiative Cooling of a Semi-infinite Solid with Parallel Walled Cavities", Int. J. Heat Mass Transfer 9, 527-532 (1966).
31. Gay, B. and Cameron, P. T., "The Efficiency of Numerical Solutions of the Heat Conduction Equation," ASME Paper No. 67-WA-HT-17.
32. Crosbie, A. L. and Viskanta, R., "Transient Heating or Cooling of a Plate by Combined Convection and Radiation", Int. J. Heat Mass Transfer 11, 305-317 (1967).
33. Adarkar, D. B. and Harstook, L. B., "Conduction with a Time-Varying Radiation Boundary Condition", Int. J. Heat Mass Transfer 10, 403-406 (1967).
34. Vardi, J. and Lemlich, R., "Radiation from and Conduction within a Finite Cylinder with a Distributed Electromagnetic Heat Source", A.I.Ch.E. - A.S.M.E., Preprint 16 (1967).
35. Vadin, Y. V., "Transient Temperature Distribution in a Slab with simultaneous Thermal Radiation and Convection", J. Eng. Physics 12, 669-671 (1967).
36. Crosbie, A. L. and Viskanta, R., "A Simplified Method for solving Transient Heat Conduction Problems with Nonlinear Boundary Conditions", J. Heat Transfer 90, 358-359 (1969).
37. Mason, C., "A Numerical Solution of the Conduction Problem with Radiating Surface", AIAA Journal 7, 2182-2184 (1969).
38. Abrams, M., "Transient Temperature Distributions in a Radiating Sphere", SC-RR-69-559A, Sandia Laboratories, Albuquerque, N.M., Sept. (1969).
39. Ayers, D. L., "The Transient Temperature Distribution in a Radiating Cylinder", Jet Propulsion Laboratory, California Institute of Technology, Research sponsored by NASA, Contract No. NAS 7-100, ASME Paper No. 67-HT-71, 1967.
40. Ayers, D. L., "Transient Cooling of a Sphere in Space", J. Heat Transfer 92, 180-182 (1970).
41. Rosen, S. S., "The Temperature Distribution in a Semi-infinite Solid with variable Thermophysical Properties subjected to Convection and/or Radiation at the Boundary", Ph.D. Dissertation, Polytechnic Institute of Brooklyn (1970).
42. Graham, J. W., "Application of a Sampled Data Model to the Transient Response of a Distributed Parameter subjected to simultaneous Thermal Radiation and Convection", Int. J. Heat Mass Transfer 13, 1636-1639 (1970).

43. Vujanovic, B., "An Approach to Linear and Nonlinear Heat Transfer Problem using a Lagrangian", AIAA Journal 9, 131-134 (1971).
44. Millet, K. B., The Cooling of Quenching Oil in the Heat Treatment of Steel, The Griscom Russel Co., New York (1927).
45. Berenson, P. J., "Experiments on Pool Boiling Heat Transfer", Int. J. Heat Mass Transfer 5, 985-999 (1962).
46. Roshenow, W. M., "Heat Transfer with Boiling", Trans. ASHRAE 72, 7-27 (1966).
47. Krieth, F., Principles of Heat Transfer, pp. 326-258, 434-477, International Text Book Co., Scranton, Penna. (1965).
48. Hsu, S. T., Engineering Heat Transfer, D. Van Nostrand Co. Inc., New York (1963).
49. Jacob, M., Heat Transfer, Vol. 1, p. 447, John Wiley & Sons Inc., New York (1964).
50. McAdams, W. H., "Heat Transfer at High Rates to Water with Surface Boiling", I and EC 41, 1945-1953 (1949).
51. Wylie, C. R., Advanced Engineering Mathematics, pp. 334-335, McGraw-Hill Book Co., New York (1960).
52. Davis, P. J. and Polonsky, I., "Numerical Interpolation, Differentiation and Integration", Handbook of Mathematical Functions N.B.S., Applied Mathematics Series 55, (Abramowitz, M. and Stegan, I. A. -ed.), U.S. Govt. Printing Office, 889 (1964).
53. Jennings, W., First Course in Numerical Methods, McMillan Co., New York (1967).
54. Schneider, P. J., Temperature Response Charts, pp. 143-149, John Wiley & Sons Inc., New York (1963).
55. Schneider, P. J., Conduction Heat Transfer, Addison Wesley Publishing Co. Inc., Reading, Mass. (1957).
56. Hildebrand, F. B., Methods of Applied Mathematics, p. 459, Prentice Hall Inc., New York (1952).
57. Bellman, R., A Brief Introduction to Theta Function, pp. 10-11, Reinhart & Winston, New York (1961).
58. Kaplan, W., Operational Methods for Linear Systems, p. 151, Addison Wesley Publishing Co., Reading, Mass. (1962).

59. Bateman, H., Tables of Integral Transformations, McGraw-Hill Book Co., New York (1952).
60. Davis, H. T. and Kirkham, W. J., "A New Table of the Zeros of the Bessel Functions  $J_0(x)$  and  $J_1(x)$  with corresponding values of  $J_1(x)$  and  $J_0(x)$ ", Bull. Amer. Math. Soc. 33, 760-772 (1927).
61. Oliver, F. W. J. (Editor), Bessel Functions, Part 3; Zeros and Associated Values, Royal Soc. Math. Tables, Vol. 7, p. XVIII, University Press, Cambridge (1960).
62. Grey, Mathews and McRoberts, A Treatise on Bessel Functions, p. 262, McMillan Co., London (1952).
63. Watson, G. N., Theory of Bessel Functions, p. 502, McMillan Co., New York, London (1944).
64. McCalla, T. R., Introduction to Numerical Methods and Fortran Programming, John Wiley & Sons Inc., New York (1967).
65. McCracken, D. D. and Dorn, W. S., Numerical Methods and Fortran Programming, p. 56, John Wiley & Sons Inc., New York (1964).

VIII VITA

Salil Kumar Bandyopadhyay (last name also known as "Banerjee") was born to Prof. Anil K. Banerjee and Mrs. Renu Banerjee on November 7, 1943 in Calcutta, India. He got his High School diploma from Mitra Institution (Bhowanipore Br.), Calcutta in First Division with distinction in June, 1959 and was awarded a scholarship on the basis of his performance. He obtained his Intermediate Science Certificate from Presidency College, Calcutta (a college in the organization of Calcutta University) in June, 1961 and was placed in the First Division. He received his "Bachelor of Mechanical Engineering degree from Jadavpur University, Calcutta in July, 1965 and was placed in the First Class. From September, 1965 to December, 1969, he was employed as a "Plant Maintenance Engineer" in The Indian Iron & Steel Co. Ltd., a steel manufacturing plant, located 140 miles southwest of Calcutta. He was enrolled as a graduate student in the University of Missouri-Rolla in January, 1970. The author intends to obtain his Ph.D. degree from the same school. At present he is employed as a Graduate Teaching Assistant in the department of Mechanical Engineering at the University of Missouri-Rolla.